

Regression Discontinuity Designs Under Interference*

Elena Dal Torrione[†] Tiziano Arduini[‡] Laura Forastiere[§]

Abstract

We extend the continuity-based framework to Regression Discontinuity Designs (RDDs) to identify and estimate causal effects in the presence of interference when units are connected through a network. In this setting, assignment to an “effective treatment”, which comprises the individual treatment and a summary of the treatment of interfering units (e.g., friends, classmates), is determined by the unit’s score and the scores of other interfering units, leading to a multiscore RDD with potentially complex, multidimensional boundaries. We characterize these boundaries and derive generalized continuity assumptions to identify the proposed causal estimands, i.e., point and boundary causal effects. Additionally, we develop a distance-based nonparametric estimator, derive its asymptotic properties under restrictions on the network degree distribution, and introduce a novel variance estimator that accounts for network correlation. Finally, we apply our methodology to the PROGRESA/Oportunidades dataset to estimate the direct and indirect effects of receiving cash transfers on children’s school attendance.

Keywords: Causal inference, regression discontinuity, interference, networks, local polynomials, statistical dependence.

*Working paper version.

[†]Department of Economics and Finance, Tor Vergata University of Rome.

[‡]Department of Economics and Finance, Tor Vergata University of Rome

[§]Department of Biostatistics, Yale University.

1 Introduction

The Regression Discontinuity Design (RDD) is widely employed in causal inference and program evaluation with non-experimental data. RDDs arise whenever a “treatment” is assigned based on whether an observed variable, known as the “score variable” or “forcing variable,” exceeds a specific cutoff. For instance, in conditional cash transfer (CCT) programs, eligibility for financial aid hinges on the household’s poverty index relative to a predetermined threshold. The deterministic nature of the RDD assignment mechanism violates the overlap assumption and prevents the use of covariate adjustment methods, common in observational studies (e.g. [Hernan and Robins, 2023](#)). However, since its early development ([Hanh et al., 2001](#); [Lee, 2008](#)), the analysis of RDDs has relied on an assumption of continuity of the outcome regression functions to allow the identification of the average treatment effect at the cutoff.

RDDs have gained renewed interest in recent years, leading to significant methodological advancements ([Calonico et al., 2019](#); [Imbens and Wager, 2019](#); [Calonico et al., 2014](#); [Kolesár and Rothe, 2018](#); [Lee and Card, 2008](#); [Hanh et al., 2001](#)). However, the issue of interference in RDDs remains largely unexplored. Interference is said to be present whenever the “treatment” on one unit affects the outcome of another unit ([Cox, 1958](#)), a common occurrence in settings where units interact physically or socially. In public health, for instance, vaccination of part of a community can indirectly protect unvaccinated members ([Halloran and Struchiner, 1995](#)). In education, student’s academic performance may be influenced by their own and peers’ retention or promotion ([Hong and Raudenbush, 2006](#)).

Interference can affect settings that can be seen and analyzed as RDDs, such as CCT programs. For instance, exploiting the randomization in the first stage of a two-stage partial population experiment, [Angelucci and De Giorgi \(2009\)](#) show that the Mexican PROGRESA/Oportunidades program increased consumption levels among ineligible households through informal loans from beneficiaries. Similarly, [Lalive and Cattaneo \(2009\)](#) find large spillover effects on the school attendance of ineligible children living in villages assigned to the program due to social interactions.

The literature on causal inference under interference has grown rapidly in recent years. Most approaches rely on structural assumptions on the interference mechanism, such as limiting interference to specified “interference sets.” A common assumption is

partial interference, which allows interference within clusters but not across clusters (Sobel, 2006). For example, partial interference is used in the study of two-stage randomized experiments to estimate treatment and spillover effects (Hudgens and Halloran, 2008; Liu and Hudgens, 2014; Baird et al., 2018). In observational studies, inverse-probability-weighted (IPW) estimators have also been derived under the partial interference assumption (Tchetgen Tchetgen and VanderWeele, 2012; Papadogeorgou et al., 2019; Perez-Heydrich et al., 2014).

Other works have analyzed more complex interference mechanisms, such as when units are connected through a network, in experimental studies (Bowers et al., 2013; Aronow and Samii, 2017; Athey et al., 2015; Leung, 2020) and observational studies (van der Laan, 2014; Ogburn and VanderWeele, 2017; Forastiere et al., 2021, 2022; Ogburn et al., 2022). Interference in such settings is often restricted to direct connections in the network graph, an assumption known as network neighborhood interference. Moreover, it is frequently assumed that individuals’ outcomes are affected by a summary measure of the treatments within the interference set specified by an “exposure mapping” (e.g., Manski, 2013; Sofrygin and van der Laan, 2017; Aronow et al., 2017; Forastiere et al., 2021). In experimental studies with general network interference, several methods of analysis have been used, such as randomization tests (Bowers et al., 2013; Athey et al., 2015), IPW type estimators (Aronow et al., 2017) and regression-based approaches (Leung, 2020). Approaches to observational studies on networks include generalized propensity score-based estimators (Forastiere et al., 2021, 2022), IPW estimators (Liu et al., 2016), targeted maximum likelihood estimator (TMLE) (Sofrygin and van der Laan, 2017; Ogburn et al., 2022) and covariate-adjustment methods based on graph neural networks (GNN) (Leung and Loupos, 2023).

This paper presents a formal framework that integrates interference into the conventional continuity-based approach to RDDs. To our knowledge, this is the first comprehensive attempt to formalize interference within RDDs. The only other work addressing interference in RDDs is Aronow et al. (2017), who study a difference-in-means estimator for the average treatment effect near the cutoff under a local randomization assumption. In contrast, we develop a general framework within the continuity-based approach and provide an identification and estimation strategy for direct and spillover effects and overall direct effects (Forastiere et al., 2021).

We begin by formalizing the problem of interference in RDDs, where potential

outcomes depend on the treatment of other units within an interference set—such as a unit’s network neighborhood (e.g. [Forastiere et al., 2021](#)) or cluster (e.g. [Sobel, 2006](#))—through an exposure mapping function (e.g. [Aronow and Samii, 2017](#)). This reduces the number of potential outcomes, which are indexed by a bivariate “effective” treatment, combining the binary individual treatment and a spillover exposure, that is, the random variable resulting from the exposure mapping.

Our framework’s key feature is that effective treatment assignment is a deterministic function of both the individual score and the scores of units within the interference set, leading to a multiscore RDD characterized by complex, multidimensional boundaries. We define new causal estimands based on these boundaries and provide identification results by extending the standard RDD continuity assumptions. In addition, we show that the traditional RDD approach identifies a meaningful overall direct effect at the cutoff, even if interference is not accounted for.

Building on the literature on multivariate RDDs ([Black, 1999](#); [Imbens and Zajonc, 2011](#); [Keele and Titiunik, 2015](#)), we propose an estimation method that reduces multivariate scores to a univariate distance measure from the boundary and uses this new variable in a local linear regression analysis. We also develop bias-corrected versions of these estimators ([Calonico et al., 2014](#)). In addition to multidimensional boundaries, another difficulty in our setting is the potential dependence in the data, given by network structures that may introduce correlations in both outcome and score variables, as well as interference sets potentially overlapping. Here, building on [Leung \(2020\)](#), we establish the asymptotic properties of our estimator under an assumption limiting the growth rate of network links and introduce a novel variance estimator that accounts for network correlation. Finally, we propose to estimate the overall direct effect at the cutoff using the canonical RDD local linear estimator. To the best of our knowledge, after [Bartalotti and Brummet \(2017\)](#) studied clustered data where all units in a cluster are on the same side of the cutoff, this is the first contribution to deal with complex dependent data in RDDs.

Our analysis is complemented by a simulation study and by an empirical illustration using data from PROGRESA/ Oportunidades, where we estimate the direct and spillover effects of the program on children’s school attendance, with interference sets defined by village, grade, and gender.

The paper is organized as follows: Section 2 introduces the notation and methodological framework; Section 3 illustrates our identifying assumptions and results; Sec-

tion 4 describes our estimation method; Section 5 includes the simulation study; Section 6 provides the empirical illustration; and Section 7 concludes.

2 Framework

2.1 Interference

Let us consider a set \mathcal{N} of n units, indexed by $i = 1, \dots, n$. Such units are connected through a set of edges, or links, \mathcal{E} with generic element $(i, j) = (j, i)$ representing the presence of a link between i and j . The pair $G = (\mathcal{N}, \mathcal{E})$ is an undirected network that can be represented by an adjacency matrix \mathbf{A} , with generic entry $A_{ij} = 1$ if unit i and j are linked and equal to 0 otherwise. Each unit is associated with a set of random variables, including a score variable $X_i \in \mathcal{X} \subseteq \mathbb{R}$, a binary treatment assignment $D_i \in \{0, 1\}$, and an outcome variable $Y_i \in \mathbb{R}$. We denote by \mathbf{X} , \mathbf{D} , and \mathbf{Y} the n -vectors collecting the score, the treatment, and the outcome variables, respectively, for all n units. Let us denote as $Y_i(\mathbf{d})$, with $\mathbf{d} \in \{0, 1\}^n$, the potential outcome we would observe on unit i if the treatment vector were set to \mathbf{d} in the sample \mathcal{N} . Because units are causally connected in this setting, in their most general form, potential outcomes depend on the complete treatment vector.

A standard assumption in causal inference, namely the “consistency” assumption, ensures that potential outcomes are well-defined by excluding the existence of multiple versions of the treatment.

Assumption 1 (Consistency). *For all $i \in \mathcal{N}$, if $\mathbf{D} = \mathbf{d}$ then $Y_i = Y_i(\mathbf{d})$.*

Consistency constitutes the first component of the so-called Stable Unit Treatment Value Assumption (SUTVA, Rubin (1986)). The critical second component of SUTVA is the no-interference assumption, under which a unit’s potential outcomes depend solely on the individual treatment. Here, we keep the consistency requirement and proceed by relaxing the conventional no-interference assumption.

For each unit $i \in \mathcal{N}$ let us define an interference set $\mathcal{S}_i \subseteq (\mathcal{N} \setminus \{i\})$ with cardinality $|\mathcal{S}_i|$. We refer to elements of \mathcal{S}_i as *neighbors* of i . Let us further define a partition of the set \mathcal{N} around unit i as $(i, \mathcal{S}_i, \mathcal{N} \setminus \{i, \mathcal{S}_i\})$. We partition the treatment assignment vector and the score vector accordingly, i.e., $\mathbf{D} = (D_i, \mathbf{D}_{\mathcal{S}_i}, \mathbf{D}_{\mathcal{N} \setminus \{i, \mathcal{S}_i\}})$ and $\mathbf{X} = (X_i, \mathbf{X}_{\mathcal{S}_i}, \mathbf{X}_{\mathcal{N} \setminus \{i, \mathcal{S}_i\}})$, with values $(d_i, \mathbf{d}_{\mathcal{S}_i}, \mathbf{d}_{\mathcal{N} \setminus \{i, \mathcal{S}_i\}})$ and $(x_i, \mathbf{x}_{\mathcal{S}_i}, \mathbf{x}_{\mathcal{N} \setminus \{i, \mathcal{S}_i\}})$,

respectively. In this partition, $\mathbf{D}_{\mathcal{S}_i}$ and $\mathbf{X}_{\mathcal{S}_i}$ collect the treatments and the score variables of units in \mathcal{S}_i , while $\mathbf{D}_{\mathcal{N}\setminus\{i,\mathcal{S}_i\}}$ and $\mathbf{X}_{\mathcal{N}\setminus\{i,\mathcal{S}_i\}}$ collect the treatments and score variables of all units not in \mathcal{S}_i and different from i .

The interference set \mathcal{S}_i may contain all units that are connected to i by a link in \mathbf{A} , i.e., the network neighborhood (network neighborhood interference, Forastiere et al. 2021). When units are grouped in clusters, such as communities, villages, and schools, \mathcal{S}_i can include only units in the same cluster as i (partial interference, Sobel 2006)¹. The interference set \mathcal{S}_i can also be defined based on network (or cluster) features and covariates. For example, in school settings, children may interact more with classmates of the same gender (Shrum et al., 1988), so that \mathcal{S}_i consists of individuals within the same school and gender group.

Additionally, we define the exposure mapping as a function that maps the treatment vector within \mathcal{S}_i to an exposure value: $g : \{0, 1\}^{|\mathcal{S}_i|} \rightarrow \mathcal{G}_i$. Let $G_i \in \mathcal{G}_i$ be the resulting random variable, with $G_i = g(\mathbf{D}_{\mathcal{S}_i})$. We refer to G_i as the *neighborhood treatment*.² Common examples of exposure mapping functions include the number or proportion of treated neighbors, $G_i = \sum_{j \in \mathcal{S}_i} D_j$ and $G_i = \frac{\sum_{j \in \mathcal{S}_i} D_j}{|\mathcal{S}_i|}$. Another type is the *one treated* exposure mapping, $G_i = \mathbb{1}\{\sum_{j \in \mathcal{S}_i} D_j > 0\}$, which takes value one if there is at least one treated unit in \mathcal{S}_i , and zero otherwise.

We introduce an interference assumption that restricts interference within interference sets and uses the exposure mapping function to describe the interference mechanism.

Assumption 2 (Interference). *For all $i \in \mathcal{N}$, and for all $\mathbf{d}, \mathbf{d}' \in \{0, 1\}^n$ such that $d_i = d'_i$ and $g(\mathbf{d}_{\mathcal{S}_i}) = g(\mathbf{d}'_{\mathcal{S}_i})$, the following holds:*

$$Y_i(d_i, \mathbf{d}_{\mathcal{S}_i}, \mathbf{d}_{\mathcal{N}\setminus\{i,\mathcal{S}_i\}}) = Y_i(d'_i, \mathbf{d}'_{\mathcal{S}_i}, \mathbf{d}'_{\mathcal{N}\setminus\{i,\mathcal{S}_i\}})$$

Assumption 2 allows potential outcomes of unit i to depend on the treatments of units within \mathcal{S}_i while precluding effects from units outside of it. Moreover, the treatments of units in \mathcal{S}_i are assumed to affect the potential outcomes of i only

¹This scenario is a particular case of neighborhood interference represented by a block-diagonal adjacency matrix.

²Observe that G_i can also be a random vector, which occurs, for example, when $g(\cdot)$ is the identity function. However, to simplify the exposition, we focus on the one-dimensional case.

through the exposure mapping. For example, if $g(\cdot)$ is the sum of treated units in \mathcal{S}_i , Assumption 2 implies that for a given number of treated neighbors, unit i 's potential outcome remains unchanged irrespective of the specific treated units.

Assumption 1 and Assumption 2 together constitute an extended version of the SUTVA under which potential outcomes can be indexed by the value of the *individual treatment* D_i and by the value of the *neighborhood treatment* G_i . The tuple (D_i, G_i) is then a bivariate treatment where D_i is the binary treatment assigned to each unit i , and G_i is a summary of the treatment vector in the interference set. Following Manski (2013), we refer to this as *effective treatment*. Thus, under Assumptions 1 and 2, $Y_i(d, g)$ denotes the potential outcome of unit i if $D_i = d$ and if $G_i = g$, i.e., if the summary of treatment vector within the interference set of i has value g through the function $g(\cdot)$ ³.

The number of potential outcomes for each unit under interference depends on the specification of the interference set and the exposure mapping. For instance, with one treated exposure mapping, G_i can only take two values, drastically reducing the number of potential outcomes. Overall, the above formulations of interference set and exposure mapping are general enough to encompass a wide range of scenarios and interference mechanisms with varying degrees of complexity. Finally, Assumption 2 implies that the interference sets and the exposure mapping are correctly specified.

Throughout the paper, we assume that the network \mathbf{A} is fixed and constant during the study; it is not affected by the treatment vector \mathbf{D} and is fully observed. This ensures that the interference sets are also observed and unaffected by the treatment. In addition, the data $(\mathbf{X}, \mathbf{D}, \{Y_i(d, g)\}_{i \in \mathcal{N}, d \in \{0,1\}, g \in \mathcal{G}_i})$ are jointly distributed according to $P(\mathbf{A})$, a data-generating distribution depending on \mathbf{A} , that is, we assume that we have access to a random draw of these variables from this distribution for our population of n connected units. Our approach, which treats potential outcomes as random variables, is commonly referred to as model-based perspective (Hernan and Robins, 2023), and is similar to Sofrygin and van der Laan (2017), Ogburn et al. (2022) and Leung and Loupos (2023), who considered an interference setting where

³Potential outcomes $Y_i(d, g)$ are well-defined only for those units whose neighborhood treatment G_i can attain the value g . We indicate this feasibility set as $V_g = \{i \in \mathcal{N} : g \in \mathcal{G}_i\}$. It is also worth noting that potential outcomes for units whose interference set is empty are not defined. In this work, we leave such potential outcomes undefined. However, other assumptions are possible, such as defining for these units outcomes of the form $Y_i(d)$.

the observed data are generated from a random process conditional on the network.

2.2 Effective treatment rule

In RDDs, the treatment is assigned to each unit according to whether or not the individual score X_i exceeds a known cutoff, denoted by c . We express the individual treatment assignment through the following *individual treatment rule*:

Assumption 3 (Individual treatment rule). *For all $i \in \mathcal{N}$*

$$D_i = \mathbb{1}(X_i \geq c) = t(X_i) \tag{1}$$

Under Assumption 3, the treatment assignment is a deterministic function of the score variable, as only units scoring above the cutoff are assigned to the treatment. In sharp RDDs, when the treatment receipt coincides with the assignment, the treatment receipt follows the same individual treatment rule as in (1) (e.g., [Hanh et al., 2001](#)). On the contrary, in fuzzy RDDs, when some units do not comply with the assignment, the treatment receipt is no longer a deterministic function of the score ([Trochim, 1984](#)). This paper focuses on the causal effect of the treatment assignment D_i , referred to as intention-to-treat effect in fuzzy settings. A fundamental implication of Assumption 3 is the following property of the individual treatment assignment.

Property 1 (Non-probabilistic individual assignment). *For all $i \in \mathcal{N}$, $\mathbb{P}(D_i = 1 \mid X_i = x_i) = 0$ for $x_i < c$ and $\mathbb{P}(D_i = 1 \mid X_i = x_i) = 1$ for $x_i \geq c$.*

With a non-probabilistic individual assignment, it is not possible to observe both treated and untreated units with the same value of the individual score X_i .

The key characteristic of our framework is that the non-probabilistic nature of the individual assignment mechanism induces a non-probabilistic assignment mechanism of effective treatment under interference. For each unit $j \in \mathcal{S}_i$, the treatment assignment is $D_j = t(X_j)$ according to Eq. (1). Therefore, G_i can be rewritten as follows:

$$G_i = g(\mathbf{D}_{\mathcal{S}_i}) = g(\{t(X_j)\}_{j \in \mathcal{S}_i}) = e(\mathbf{X}_{\mathcal{S}_i}) \tag{2}$$

We refer to $e(\mathbf{X}_{\mathcal{S}_i})$ as the *neighborhood treatment rule*. Combining the individual and the neighborhood treatment rule, we obtain a deterministic vector-valued *effective treatment rule*:

$$(D_i, G_i) = (t(X_i), e(\mathbf{X}_{S_i})) = \mathbf{F}(X_i, \mathbf{X}_{S_i}) \quad (3)$$

From Eq. (3), it is clear that the effective treatment is governed by multiple scores. Therefore, RDDs under interference can be reframed as a “multiscore design” (Reardon and Robinson, 2012; Wong et al., 2013). It is worth noting, however, that in typical multiscore RDDs, the individual treatment is assigned based on multiple individual scores (e.g., math and reading test scores, Matsudaira, 2008). Here, on the other hand, the first component of the effective treatment, i.e., the individual treatment D_i , is determined by the individual score, which is assumed to be a one-dimensional variable X_i , and the second component, i.e., the neighborhood treatment G_i , is determined by the scores of units in the interference set \mathbf{X}_{S_i} . Thus, the effective treatment is determined by multiple scores of the same variable on different units.

Let us define the multiscore space $\mathcal{X}_{iS_i} \subseteq \mathbb{R}^{|\mathcal{S}_i|+1}$ as the space of all elements (x_i, \mathbf{x}_{S_i}) . The effective treatment rule defines a partition of \mathcal{X}_{iS_i} into *effective treatment regions*, defined as

$$\mathcal{X}_{iS_i}(d, g) = \{(x_i, \mathbf{x}_{S_i}) \in \mathcal{X}_{iS_i} : \mathbf{F}(x_i, \mathbf{x}_{S_i}) = (d, g)\}$$

where the probability of receiving the effective treatment (d, g) is equal to one. Formally, we can state the following property of RDDs under interference, characterized by a non-probabilistic individual treatment assignment (Property 1) and an interference mechanism defined in Assumption 2.

Property 2 (Non-probabilistic effective treatment assignment). *For all $i \in \mathcal{N}$, for all $d \in \{0, 1\}$, and for all $g \in \mathcal{G}_i$*

$$\mathbb{P}(D_i = d, G_i = g | (X_i, \mathbf{X}_{S_i}) = (x_i, \mathbf{x}_{S_i})) = \begin{cases} 1 & (x_i, \mathbf{x}_{S_i}) \in \mathcal{X}_{iS_i}(d, g) \\ 0 & (x_i, \mathbf{x}_{S_i}) \notin \mathcal{X}_{iS_i}(d, g) \end{cases}$$

Property 2 implies that conditional on (X_i, \mathbf{X}_{S_i}) potential outcomes are independent of the effective treatment, as stated in the following property.

Property 3 (Unconfoundedness). *For all $i \in \mathcal{N}$, for all $d \in \{0, 1\}$ and for all $g \in \mathcal{G}_i$*

$$Y_i(d, g) \perp\!\!\!\perp D_i, G_i | X_i, \mathbf{X}_{S_i}$$

In other words, under Assumptions 2 and 3 (implying Property 2), unconfoundedness holds conditional on the individual score X_i and the scores within the interference set \mathbf{X}_{S_i} . Conditional unconfoundedness, then, is an inherent characteristic of the RDD with interference under Assumption 2 resulting from the deterministic dependence of the effective treatment on (X_i, \mathbf{X}_{S_i}) .

2.3 Effective treatment boundaries

The non-probabilistic effective treatment assignment results in a structural lack of overlap, as units with the same value of (X_i, \mathbf{X}_{S_i}) are never observed under different effective treatments. Therefore, unconfoundedness cannot be exploited directly as in other observational studies with interference (van der Laan, 2014; Papadogeorgou et al., 2019; Perez-Heydrich et al., 2014; Ogburn et al., 2022; Forastiere et al., 2021, 2022). However, in analogy to RDDs without interference, if the potential outcome regression functions are continuous in (X_i, \mathbf{X}_{S_i}) , causal effects can be identified at common boundary points between effective treatment regions using units whose score values are sufficiently close to such points. This is only feasible if the regions share at least one boundary point.

Let the common boundary points between effective treatment regions $\mathcal{X}_{iS_i}(d, g)$ and $\mathcal{X}_{iS_i}(d', g')$ be denoted by $\bar{\mathcal{X}}_{iS_i}(d, g | d', g')$. We refer to this set as the *effective treatment boundary*. Furthermore, define $\mathcal{D}_{iS_i} \subseteq \{0, 1\}^{|S_i|+1}$ as the space of the elements (d_i, \mathbf{d}_{S_i}) , and let $\mathcal{D}_{iS_i}(d, g) = \{(d_i, \mathbf{d}_{S_i}) \in \mathcal{D}_{iS_i} \text{ s.t. } (d_i, g(\mathbf{d}_{S_i})) = (d, g)\}$, with generic element $(d_i^{d,g}, \mathbf{d}_{S_i}^{d,g})$. The following theorem provides a procedure to characterize the effective treatment boundary between any two effective treatment regions of interest.

Theorem 1 (Characterization of effective treatment boundaries). *Let $g : \{0, 1\}^{|S_i|} \rightarrow \mathcal{G}_i$ be a generic exposure mapping and suppose Assumption 3 holds. Consider two distinct effective treatments (d, g) and (d', g') with $d, d' \in \{0, 1\}$ and $g, g' \in \mathcal{G}_i$, and let $(d_i^{d,g}, \mathbf{d}_{S_i}^{d,g})$ and $(d_i^{d',g'}, \mathbf{d}_{S_i}^{d',g'})$ be two generic points in $\mathcal{D}_{iS_i}(d, g)$ and $\mathcal{D}_{iS_i}(d', g')$. Select a point $(x_i^*, \mathbf{x}_{S_i}^*) \in \mathcal{X}_{iS_i}$ such that for all $z \in (\{i\} \cup S_i)$: $x_z^* \geq c$ if $d_z^{d,g} = d_z^{d',g'} = 1$; $x_z^* \leq c$ if $d_z^{d,g} = d_z^{d',g'} = 0$; $x_z^* = c$ if $d_z^{d,g} \neq d_z^{d',g'}$. Then $(x_i^*, \mathbf{x}_{S_i}^*) \in \bar{\mathcal{X}}_{iS_i}(d, g | d', g')$. Furthermore, any point in $\bar{\mathcal{X}}_{iS_i}(d, g | d', g')$ can be obtained using this procedure.*

Proof. See Supplementary Material S.1..

Corollary 1. *Under the assumptions of Theorem 1 for any $d, d' \in \{0, 1\}$ and $g, g' \in \mathcal{G}_i$:*

1. *Every point in $\bar{\mathcal{X}}_{i\mathcal{S}_i}(d, g | d', g')$ has at least one coordinate that is equal to the cutoff c .*
2. *The point in $\mathcal{X}_{i\mathcal{S}_i}$ where all coordinates are equal to c is an element of $\bar{\mathcal{X}}_{i\mathcal{S}_i}(d, g | d', g')$.*

Theorem 1 characterizes the effective treatment boundary between any two treatment regions. This is relevant because determining common boundary points might be challenging when the exposure mapping functions are complex, as different exposure mapping functions generate different partitions of the multiscore space. Additionally, Corollary 1 establishes two key properties. First, every point on the effective treatment boundary has at least one coordinate equal to the cutoff. Second, the subset $\bar{\mathcal{X}}_{i\mathcal{S}_i}(d, g | d', g')$ is always non-empty, as it includes the point having all coordinates equal to c , guaranteeing the identification of causal effects at least at one point in the multiscore space, regardless of the complexity of the interference mechanism.

Figure 1 and Figure 2 illustrate the concepts expressed so far, including how different exposure mapping functions lead to different effective treatment regions and boundaries.

In the scenario depicted in Figure 1 each unit has one neighbor, $\mathcal{S}_i = \{j\}$, and $G_i = D_j$. The multiscore space $\mathcal{X}_{i\mathcal{S}_i}$ is represented on the Cartesian plane where X_i is on the x -axis and X_j on the y -axis. Note that if $X_i \geq c$ then $D_i = 1$ and if $X_i < c$ then $D_i = 0$. Similarly, if $X_j \geq c$ then $D_j = G_i = 1$, and if $X_j < c$ then $D_j = G_i = 0$. This leads to a partition of the multiscore space into four distinct effective treatment regions where the effective treatment boundary is either a segment (for example, between the top-left and the bottom-left effective treatment regions) or the point (c, c) (between the bottom-left and top-right effective treatment regions).

Figure 2 compares the scenario where each unit has two neighbors, $\mathcal{S}_i = \{j, k\}$ with one treated exposure mapping (Figure 2.a) against the scenario with $\mathcal{S}_i = \{j, k\}$ and “sum of treated” exposure mapping. In principle, the complete multiscore space $\mathcal{X}_{i\mathcal{S}_i}$ is three-dimensional. For ease of representation, we only represent effective treatment regions for $D_i = 0$ by fixing X_i at a level x_i with $x_i < c$. With the one treated exposure mapping and $D_i = 0$, there are two effective treatment regions, i.e., $\mathcal{X}_{i\mathcal{S}_i}(0, 0)$ and $\mathcal{X}_{i\mathcal{S}_i}(0, 1)$, and the effective treatment boundary is given by the two intersecting segments in solid black line. With the “sum of treated” exposure

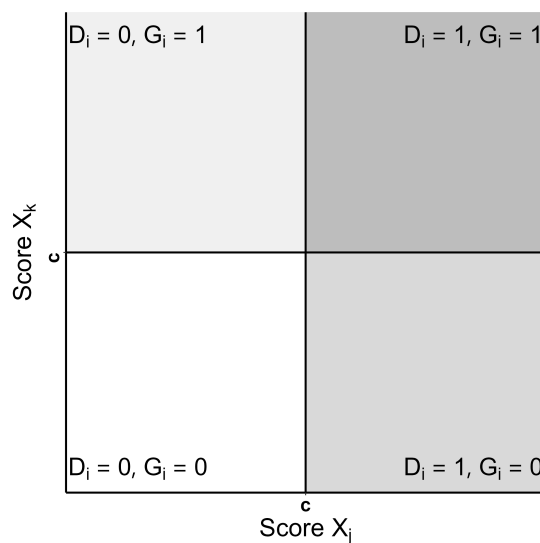


Figure 1: Score space for unit i with interference set $\mathcal{S}_i = \{j\}$ and $G_i = D_j$.

mapping, (for $D_i = 0$) there are three effective treatment regions that are separated pairwise by segments, except for regions $\mathcal{X}_{i\mathcal{S}_i}(0, 2)$ and $\mathcal{X}_{i\mathcal{S}_i}(0, 0)$, where the treatment boundary is given by (c, c) .

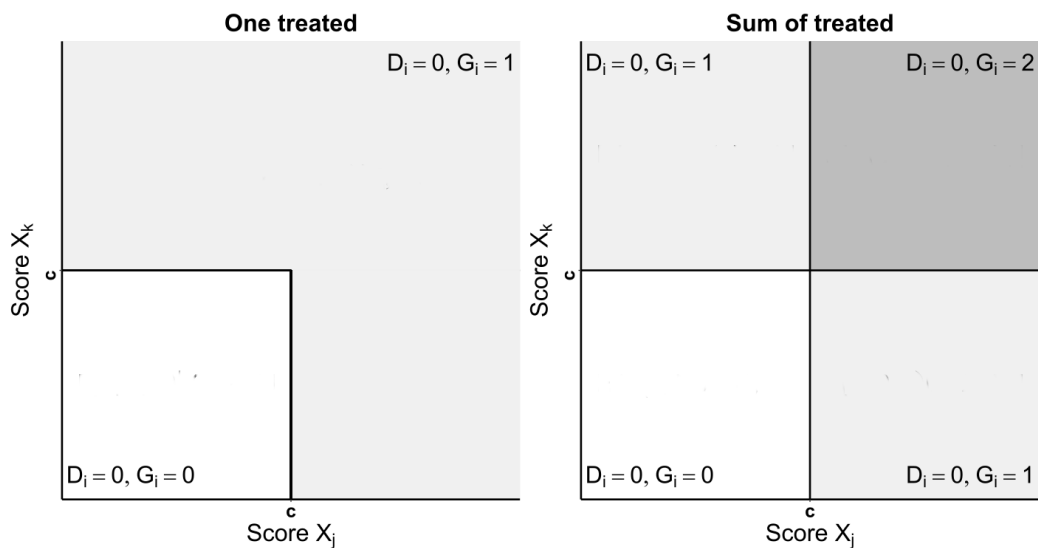


Figure 2: Score space for unit i with interference set $\mathcal{S}_i = \{j, k\}$ fixing $X_i = x_i$ with $x_i < c$.

2.4 Causal Estimands

In the remainder of the paragraph, for simplicity, we will concentrate on scenarios where all interference sets exhibit a uniform cardinality $|\mathcal{S}_i| = S$. The first causal estimand of interest is the *boundary point average causal effect*, the difference between average potential outcomes under different effective treatments (d, g) and (d', g') at a point of the effective treatment boundary $\bar{\mathcal{X}}_{i\mathcal{S}_i}(d, g | d', g')$:

$$\tau_{d,g|d',g'}(\bar{x}_i, \bar{\mathbf{x}}_{\mathcal{S}_i}) = \mathbb{E}[Y_i(d, g) - Y_i(d', g') | (X_i, \mathbf{X}_{\mathcal{S}_i}) = (\bar{x}_i, \bar{\mathbf{x}}_{\mathcal{S}_i})] \quad (4)$$

with $d, d' \in \{0, 1\}$, $g, g' \in \mathcal{G}_i$, $(\bar{x}_i, \bar{\mathbf{x}}_{\mathcal{S}_i}) \in \bar{\mathcal{X}}_{i\mathcal{S}_i}(d, g | d', g')$. Here, the expectation is taken with respect to the distribution of potential outcomes conditional on the individual and neighborhood score and the observed network under our model-based perspective. Theoretically, point average causal effects could be defined for any point on the multiscore space. However, due to the lack of overlap entailed by Property 2, such effects can only be identified at points in the effective treatment boundary $\bar{\mathcal{X}}_{i\mathcal{S}_i}(d, g | d', g')$ under minimal continuity assumptions, as shown in the next section.

The second estimand of interest is the *boundary average causal effects*, the difference in the average potential outcomes under different effective treatments at the entire effective treatment boundary:

$$\tau_{d,g|d',g'}(\bar{\mathcal{X}}_{i\mathcal{S}_i}(d, g | d', g')) = \mathbb{E}[Y_i(d, g) - Y_i(d', g') | (X_i, \mathbf{X}_{\mathcal{S}_i}) \in \bar{\mathcal{X}}_{i\mathcal{S}_i}(d, g | d', g')] \quad (5)$$

with $d \in \{0, 1\}$, $g, g' \in \mathcal{G}_i$. Boundary average causal effects are weighted averages of boundary point average causal effects across the effective treatment boundary:

$$\tau_{d,g|d',g'}(\bar{\mathcal{X}}_{i\mathcal{S}_i}(d, g | d', g')) = \int_{\bar{\mathcal{X}}_{i\mathcal{S}_i}(d, g | d', g')} \tau_{d,g|d',g'}(x_i, \mathbf{x}_{\mathcal{S}_i}) f(x_i, \mathbf{x}_{\mathcal{S}_i} | (X_i, \mathbf{X}_{\mathcal{S}_i}) \in \bar{\mathcal{X}}_{i\mathcal{S}_i}(d, g | d', g')) d(x_i, \mathbf{x}_{\mathcal{S}_i}) \quad (6)$$

where $f(x_i, \mathbf{x}_{\mathcal{S}_i})$ is the joint density of X_i and $\mathbf{X}_{\mathcal{S}_i}$. We further distinguish between direct and indirect average causal effects. Specifically, we define *boundary point direct effects* and *boundary direct effects* as follows:

$$\begin{aligned} \tau_{1,g|0,g}(\bar{x}_i, \bar{\mathbf{x}}_{\mathcal{S}_i}) &= \mathbb{E}[Y_i(1, g) - Y_i(0, g) | (X_i, \mathbf{X}_{\mathcal{S}_i}) = (\bar{x}_i, \bar{\mathbf{x}}_{\mathcal{S}_i})] \\ \tau_{1,g|0,g}(\bar{\mathcal{X}}_{i\mathcal{S}_i}(1, g | 0, g)) &= \mathbb{E}[Y_i(1, g) - Y_i(0, g) | (X_i, \mathbf{X}_{\mathcal{S}_i}) \in \bar{\mathcal{X}}_{i\mathcal{S}_i}(1, g | 0, g)] \end{aligned} \quad (7)$$

for $g \in \mathcal{G}_i$ and $(\bar{x}_i, \bar{\mathbf{x}}_{S_i}) \in \bar{\mathcal{X}}_{iS_i}(1, g|0, g)$. These effects isolate the (local) impact of the individual treatment for a fixed level of G_i . In contrast, *boundary point* and *boundary indirect effects* capture the indirect effects of changing the neighborhood treatment G_i for a fixed level of the individual treatment:

$$\begin{aligned}\tau_{d,g|d,g'}(\bar{x}_i, \bar{\mathbf{x}}_{S_i}) &= \mathbb{E}[Y_i(d, g) - Y_i(d, g') | (X_i, \mathbf{X}_{S_i}) = (\bar{x}_i, \bar{\mathbf{x}}_{S_i})] \\ \tau_{d,g|d,g'}(\bar{\mathcal{X}}_{iS_i}(d, g|d, g')) &= \mathbb{E}[Y_i(d, g) - Y_i(d, g') | (X_i, \mathbf{X}_{S_i}) \in \bar{\mathcal{X}}_{iS_i}(d, g|d, g')]\end{aligned}\quad (8)$$

for $d \in \{0, 1\}$, $g, g' \in \mathcal{G}_i$ and $\bar{x}_i, \bar{\mathbf{x}}_{S_i} \in \bar{\mathcal{X}}_{iS_i}(d, g|d, g')$.

Finally, we define the *boundary overall direct effect* as

$$\tau_{1|0} = \sum_{g \in \mathcal{G}_i} \tau_{1,g|0,g}(\bar{\mathcal{X}}_{iS_i}(1, g|0, g)) \cdot \mathbb{P}(G_i = g | X_i = c) \quad (9)$$

which averages boundary direct effects over the probability distribution of G_i conditional on X_i being equal to the cutoff. This effect can be written as a weighted average of boundary point direct effects across the union of all boundaries of the type $\bar{\mathcal{X}}_{iS_i}(1, g|0, g)$ ⁴. Thus, the boundary overall direct effect summarizes the effect of the individual treatment at the cutoff⁵. In the example shown in Figure 1, the overall direct effect at the cutoff corresponds to the boundary point direct effects averaged along the whole line $X_i = c$, which is the union of the boundaries $\bar{\mathcal{X}}_{iS_i}(1, 1|0, 1)$ and $\bar{\mathcal{X}}_{iS_i}(1, 0|0, 0)$. We note that our definitions of causal effects assume homogeneity of $\mathbb{E}[Y_i(d, g) | (X_i, \mathbf{X}_{S_i}) = (x_i, \mathbf{x}_{S_i})]$ and $f(x_i, \mathbf{x}_{S_i})$ across units. This assumption may be strong, as the outcome and score distributions may depend on the observed net-

⁴Specifically, $\bar{\mathcal{X}}_{iS_i}(1, g|0, g) = \{(x_i, \mathbf{x}_{S_i}) \in \mathcal{X}_{iS_i} : x_i = c, \mathbf{x}_{S_i} \in \mathcal{X}_{S_i}(g)\}$ where $\mathcal{X}_{S_i}(g)$ is the set of all elements \mathbf{x}_{S_i} such that $e(\mathbf{x}_{S_i}) = g$. This follows from an application of Theorem 1. The union of all such boundaries across g then corresponds to $\{(x_i, \mathbf{x}_{S_i}) \in \mathcal{X}_{iS_i} : x_i = c\}$. Noting that $\mathbb{P}(G_i = g | X_i = c) = \mathbb{P}((X_i, \mathbf{X}_{S_i}) \in \bar{\mathcal{X}}_{iS_i}(1, g|0, g) | X_i = c)$, $\tau_{1|0}$ can be equivalently rewritten as

$$\begin{aligned}\tau_{1|0} &= \sum_{g \in \mathcal{G}_i} \tau_{1,g|0,g}(\bar{\mathcal{X}}_{iS_i}(1, g|0, g)) \cdot \mathbb{P}((X_i, \mathbf{X}_{S_i}) \in \bar{\mathcal{X}}_{iS_i}(1, g|0, g) | X_i = c) \\ &= \sum_{g \in \mathcal{G}_i} \int_{\mathcal{X}_{S_i}(g)} \mathbb{E}[Y_i(1, g) - Y_i(0, g) | X_i = c, \mathbf{X}_{S_i} = \mathbf{x}_{S_i}] \cdot \frac{f(c, \mathbf{x}_{S_i})}{f(c)} d\mathbf{x}_{S_i}\end{aligned}$$

⁵The boundary overall direct effect is similar to the overall main effect defined by [Forastiere et al. \(2021\)](#), which is the average causal effect of the individual treatment marginalized over the (empirical) probability distribution of G_i . Here, however, the boundary overall direct effect is an average of boundary (conditional) direct effects over the probability distribution of G_i at the cutoff.

work. This could happen when units have varying numbers of network connections and interference sets of different sizes. When the outcome conditional expectations are heterogeneous across units, causal estimands should be defined as the average of expected potential outcomes across the population units (e.g. [Ogburn et al., 2022](#)). We extend our analysis to account for irregularly-sized interference sets and heterogeneous outcome conditional expectations and score distributions in the online Appendix A, where we also discuss the implications for identification and estimation.

3 Identification

3.1 Identification of the boundary point and boundary average causal effects

We first introduce the following notation to formalize our identification results, which we adapt from [Imbens and Zajonc \(2011\)](#).

Let $l(p, q)$ be the Euclidean distance between two generic points p and q . We denote the ϵ -neighborhood around a generic point $(\bar{x}_i, \bar{\mathbf{x}}_{S_i}) \in \mathcal{X}_{iS_i}$ as

$$\mathcal{B}_\epsilon(\bar{x}_i, \bar{\mathbf{x}}_{S_i}) = \{(x_i, \mathbf{x}_{S_i}) \in \mathcal{X}_{iS_i} : l((x_i, \mathbf{x}_{S_i}), (\bar{x}_i, \bar{\mathbf{x}}_{S_i})) \leq \epsilon\}$$

for $\epsilon > 0$. Hence, $\mathcal{B}_\epsilon(\bar{x}_i, \bar{\mathbf{x}}_{S_i})$ contains all points in a neighborhood of radius ϵ around $(\bar{x}_i, \bar{\mathbf{x}}_{S_i})$. Let us then denote by $\mathcal{B}_{\epsilon, d, g | d', g'}(\bar{x}_i, \bar{\mathbf{x}}_{S_i})$ a neighborhood of radius ϵ around $(\bar{x}_i, \bar{\mathbf{x}}_{S_i})$, for $(\bar{x}_i, \bar{\mathbf{x}}_{S_i}) \in \bar{\mathcal{X}}_{iS_i}(d, g | d', g')$. Moreover, define the minimum distance of a point $(x_i, \mathbf{x}_{S_i}) \in \mathcal{X}_{iS_i}$ from the effective treatment boundary $\bar{\mathcal{X}}_{iS_i}(d, g | d', g')$ as $l_{d, g | d', g'}^{min}(x_i, \mathbf{x}_{S_i}) = \min_{(\bar{x}_i, \bar{\mathbf{x}}_{S_i}) \in \bar{\mathcal{X}}_{iS_i}(d, g | d', g')} l((x_i, \mathbf{x}_{S_i}), (\bar{x}_i, \bar{\mathbf{x}}_{S_i}))$, and let

$$\mathcal{B}_\epsilon(\bar{\mathcal{X}}_{iS_i}(d, g | d', g')) = \{(x_i, \mathbf{x}_{S_i}) \in \mathcal{X}_{iS_i} : l_{d, g | d', g'}^{min}(x_i, \mathbf{x}_{S_i}) \leq \epsilon\}$$

be the ϵ -neighborhood of the effective treatment boundary $\bar{\mathcal{X}}_{iS_i}(d, g | d', g')$, i.e., the set of points that are at a distance from $\bar{\mathcal{X}}_{iS_i}(d, g | d', g')$ no greater than ϵ .

We now take the intersections of the ϵ -neighborhood of a boundary point $\mathcal{B}_{\epsilon, d, g | d', g'}(\bar{x}_i, \bar{\mathbf{x}}_{S_i})$ and the ϵ -neighborhood of the effective treatment boundary $\mathcal{B}_{\epsilon, d, g | d', g'}(\bar{x}_i, \bar{\mathbf{x}}_{S_i})$ with the two effective treatment regions of interest $\mathcal{X}_{iS_i}(d, g)$ and $\mathcal{X}_{iS_i}(d', g')$. Let $\mathcal{B}_{\epsilon, d, g | d', g'}^{d, g}(\bar{x}_i, \bar{\mathbf{x}}_{S_i}) = \mathcal{B}_{\epsilon, d, g | d', g'}(\bar{x}_i, \bar{\mathbf{x}}_{S_i}) \cap \mathcal{X}_{iS_i}(d, g)$ and

$\mathcal{B}_{\epsilon, d, g | d', g'}^{d', g'}(\bar{x}_i, \bar{\mathbf{x}}_{S_i}) = \mathcal{B}_{\epsilon, d, g | d', g'}(\bar{x}_i, \bar{\mathbf{x}}_{S_i}) \cap \mathcal{X}_{iS_i}(d', g')$. We refer to the latter as left ϵ -neighborhood and the former as right ϵ -neighborhood. Similarly, let $\mathcal{B}_{\epsilon}^{d, g}(\bar{\mathcal{X}}_{iS_i}(d, g | d', g')) = \mathcal{B}_{\epsilon}(\bar{\mathcal{X}}_{iS_i}(d, g | d', g')) \cap \mathcal{X}_{iS_i}(d, g)$ and $\mathcal{B}_{\epsilon}^{d', g'}(\bar{\mathcal{X}}_{iS_i}(d, g | d', g')) = \mathcal{B}_{\epsilon}(\bar{\mathcal{X}}_{iS_i}(d, g | d', g')) \cap \mathcal{X}_{iS_i}(d', g')$

We impose the following identifying assumptions.

Assumption 4 (Identification). *Assume that (X_i, \mathbf{X}_{S_i}) has bounded support. For all $i \in \mathcal{N}$, for all $d, d' \in \{0, 1\}$ and for all $g, g' \in \mathcal{G}_i$:*

- a) (Score density positivity) *For all $(\bar{x}_i, \bar{\mathbf{x}}_{S_i}) \in \bar{\mathcal{X}}_{iS_i}(d, g | d', g')$ and $\epsilon > 0$, the marginal density $f(x_i, \mathbf{x}_{S_i})$ is strictly positive for all $(x_i, \mathbf{x}_{S_i}) \in \mathcal{B}_{\epsilon, d, g | d', g'}(\bar{x}_i, \bar{\mathbf{x}}_{S_i})$.*
- b) (Outcome continuity) *$\mathbb{E}[Y_i(d, g) | (X_i, \mathbf{X}_{S_i}) = (x_i, \mathbf{x}_{S_i})]$ is continuous at all $(x_i, \mathbf{x}_{S_i}) \in \mathcal{X}_{iS_i}$.*
- c) (Score density continuity) *$f(x_i, \mathbf{x}_{S_i})$ is continuous at all $(x_i, \mathbf{x}_{S_i}) \in \mathcal{X}_{iS_i}$.*
- d) (Outcome and score density boundedness) *$|\mathbb{E}[Y_i(d, g) | (X_i, \mathbf{X}_{S_i}) = (x_i, \mathbf{x}_{S_i})]|$ and $f(x_i, \mathbf{x}_{S_i})$ are bounded.*

Combined with the extended SUTVA (Assumptions 1 and 2) and the RDD treatment assignment rule (Assumption 1), Assumption 4 enables the identification of average causal effects at specific points of the effective treatment boundary and along the entire treatment boundary, as shown in the following theorem.

Theorem 2 (Identification). *Suppose assumptions 1-3 hold. If 4.a) and 4.b) hold, then for all $d, d' \in \{0, 1\}$, $g, g' \in \mathcal{G}_i$, and for all $(\bar{x}_i, \bar{\mathbf{x}}_{S_i}) \in \bar{\mathcal{X}}_{iS_i}(d, g | d', g')$*

$$\begin{aligned} \tau_{d, g | d', g'}(\bar{x}_i, \bar{\mathbf{x}}_{S_i}) &= \lim_{\epsilon \rightarrow 0} \mathbb{E}[Y_i | (X_i, \mathbf{X}_{S_i}) \in \mathcal{B}_{\epsilon, d, g | d', g'}^{d, g}(\bar{x}_i, \bar{\mathbf{x}}_{S_i})] \\ &\quad - \lim_{\epsilon \rightarrow 0} \mathbb{E}[Y_i | (X_i, \mathbf{X}_{S_i}) \in \mathcal{B}_{\epsilon, d, g | d', g'}^{d', g'}(\bar{x}_i, \bar{\mathbf{x}}_{S_i})] \end{aligned} \quad (10)$$

Furthermore, if also 4.c)-4.d) hold then

$$\begin{aligned} \tau_{d, g | d', g'}(\bar{\mathcal{X}}_{iS_i}(d, g | d', g')) &= \lim_{\epsilon \rightarrow 0} \mathbb{E}[Y_i | (X_i, \mathbf{X}_{S_i}) \in \mathcal{B}_{\epsilon}^{d, g}(\bar{\mathcal{X}}_{iS_i}(d, g | d', g'))] \\ &\quad - \lim_{\epsilon \rightarrow 0} \mathbb{E}[Y_i | (X_i, \mathbf{X}_{S_i}) \in \mathcal{B}_{\epsilon}^{d', g'}(\bar{\mathcal{X}}_{iS_i}(d, g | d', g'))] \end{aligned} \quad (11)$$

Theorem 2 states that the boundary point average causal effect is identified as the difference in the limits of the observed outcome expectations conditional on the right

and left ϵ -neighborhood of such point as ϵ approaches zero. This result relies on Assumptions 4.a and 4.b. Assumption 4.a requires that the joint score density is non-null in a ϵ -neighborhood of the treatment boundary point, ensuring well-defined conditional expectations of outcomes near the effective treatment boundary point. Assumption 4.b) extends the continuity requirement from standard univariate and multivariate RDDs to the interference case. This condition enables the approximation of unobserved potential outcome expectations at a boundary point using sufficiently close observations, thereby restoring a form of overlap.

Moreover, the boundary average causal effect $\tau_{d,g|d',g'}(\bar{\mathcal{X}}_{iS_i}(d, g | d', g'))$ is identified by taking the difference between the limits of the conditional expectations of the observed outcomes on $\mathcal{B}_\epsilon^{d,g}(\bar{\mathcal{X}}_{iS_i}(d, g | d', g'))$ and $\mathcal{B}_\epsilon^{d',g'}(\bar{\mathcal{X}}_{iS_i}(d, g | d', g'))$ as ϵ shrinks to zero under the additional assumptions 4.c and 4.d. Specifically, because boundary effects are weighted averages of points effects with weights determined by scores density, Assumption 4.c) ensures that the weighting scheme is also continuous on each side of the effective treatment boundary. This guarantees that a change in the distribution of the baseline score variables does not spuriously determine the difference in the potential outcomes conditional expectations. Finally, Assumption 4.d) is a technical condition allowing the interchange of the limit and integral operators.

It is worth noting that our identification result in Theorem 2, in addition to the extended SUTVA and Assumption 4, relies on the non-probabilistic treatment assignment (Property 2), entailed by Assumption 3. Such property implies a general unconfoundedness assumption conditional on the individual score and the vector of scores in the interference set (Property 3). One might replace this general unconfoundedness assumption with a weaker version conditional on some summary statistics of the scores of the interference set instead of the complete vector. However, this assumption rests on the correct choice of such summary statistics and may be prone to its misspecification. We leave the identification implications and the development of an estimator under such assumption to future work.

3.2 Identification of the boundary overall direct effect

In standard no-interference RDDs, the local average causal effect at the cutoff is identified as the difference between the right and left limit of the observed outcome regression functions as X_i approaches the cutoff c . In our framework, such an identi-

fication strategy does not identify the average causal effect at the cutoff as potential outcomes of the form $Y_i(1)$ and $Y_i(0)$ are ill-defined under interference. However, the following theorem shows that the identification strategy used in standard RDDs identifies the boundary overall direct effect at the cutoff provided that Assumptions 1-4 hold.

Theorem 3 (Identification of boundary overall direct effect). *Under assumptions 1-4*

$$\tau_{1|0} = \lim_{x_i \downarrow c} \mathbb{E}[Y_i | X_i = x_i] - \lim_{x_i \uparrow c} \mathbb{E}[Y_i | X_i = x_i]$$

Proof. See Supplementary Material S.1.

$\lim_{x_i \downarrow c} \mathbb{E}[Y_i | X_i = x_i] - \lim_{x_i \uparrow c} \mathbb{E}[Y_i | X_i = x_i]$ is precisely the quantity that identifies the average treatment effect at the cutoff in the standard RDD without interference. This result crucially relies on Assumption 4.c (score density continuity), which ensures that the distribution of \mathbf{X}_{S_i} conditional on X_i is balanced on each side of the cutoff c . This, in turn, implies that the (conditional) distribution of G_i is equal on each side of the cutoff.

In RDDs, the quantity $\lim_{x_i \downarrow c} \mathbb{E}[Y_i | X_i = x_i] - \lim_{x_i \uparrow c} \mathbb{E}[Y_i | X_i = x_i]$ is typically estimated using local polynomial regression (e.g., Hanh et al., 2001). However, contrary to typical RDD applications, where observations are assumed to be i.i.d., the data may exhibit statistical dependence in our setting due to interference and network correlation. In Section 4, we show that the conventional RDD local polynomial estimator is consistent for $\tau_{1|0}$ under an assumption limiting the “amount” of such dependence. This means that even when interference is erroneously ruled out, the resulting estimate of the conventional approach has a causal interpretation as an overall direct effect at the cutoff.

4 Estimation

This section addresses the estimation of two causal estimands introduced in section 3: the boundary average effects, $\tau_{d,g|d',g'}(\bar{\mathcal{X}}_{iS_i}(d, g | d', g'))$, and the boundary overall direct effect, $\tau_{1|0}$.

In no-interference RDDs, the average causal effect at the cutoff is typically estimated using local polynomial regression, which fits Y_i on a low-order polynomial of

the centered score ($X_i - c$) on each side of the cutoff using observations within a fixed bandwidth h_n (Hanh et al., 2001). However, estimating boundary average effects in our setting is more complex due to the multidimensional nature of the effective treatment boundaries.

Several estimation strategies for multiple scores RDDs without interference have been proposed to estimate causal effects along treatment boundaries. (Imbens and Zajonc, 2011) proposed to first estimate point effects by multiple local linear regression and integrate them numerically over the treatment boundary. Alternatively, several methods have been proposed to estimate boundary effects directly. These include response surface estimation, which fits a parametric model to the entire response surface (Reardon and Robinson, 2012), and methods that reduce the multivariate score to a one-dimensional variable and then apply univariate local polynomial techniques using this one-dimensional variable as the one-dimensional score. This is done either by subsetting the data by treatment region (frontier estimation) (Wong et al., 2013; Matsudaira, 2008) or by computing a summary score (binding approach) (Reardon and Robinson, 2012). Another popular estimation method of this class relies on the distance to the nearest boundary point (Black, 1999; Dell, 2010; Keele and Titunik, 2015). This approach reduces the multivariate score to a one-dimensional variable by computing the shortest Euclidean distance of each observation to the treatment boundary.

The distance-based method has several advantages. Unlike frontier estimation, it estimates effects over the entire treatment boundary without subsetting the data. Moreover, it can be applied to a broader range of treatment boundaries, unlike the binding approach. Lastly, its local non-parametric approach potentially avoids the misspecification pitfalls of a global model and retains the visually appealing properties of univariate RDDs (Imbens and Zajonc, 2011).

Building on this method, we propose to use a distance-based local polynomial estimator to estimate boundary average effects, motivated by the non-standard complexity of the effective treatment boundaries. Our approach simplifies the dimensionality of multiscore spaces by converting the multidimensional scores, comprising the individual and neighborhood scores, into a one-dimensional variable. For the boundary overall direct effect, $\tau_{1|0}$, we propose using the standard RDD local polynomial estimator, as justified by our identification result in Theorem 3. We also develop bias-corrected versions of these estimators, following current practices in RDDs (Calonico

et al., 2014).

Another difficulty in our setting is the potential dependence in the data. Interference can induce dependence among observations with overlapping interference sets, and network structures may introduce correlations in both outcome and score variables. For example, in network data, linked observations tend to be more similar, a phenomenon known as homophily (McPherson et al., 2001; Jackson, 2008; Christakis and Fowler, 2009). Standard asymptotic theories for local polynomial estimators, which assume i.i.d. data, are not applicable in the presence of such dependence.

The literature on dependent data in RDDs is limited. Bartalotti and Brummet (2017) addresses clustered data where all units in a cluster are on the same side of the cutoff. Results on local polynomial estimators with time-dependent and spatially-dependent data are also available (see for example, Opsomer et al., 2001; Masry and Fan, 1997; Jenish, 2012), although not explicitly developed for RDDs. However, these approaches often rely on random fields indexed by Euclidean lattices, which may not be suitable to network structures as a generic network is not necessarily embeddable in an Euclidean lattice (Kojevnikov et al., 2021). To address such network dependence, we develop a novel asymptotic theory building on Leung (2020), establishing the asymptotic normality of our estimators under a condition that limits the growth of network links.

4.1 Potential outcome model

We consider the following model for the potential outcomes:

Assumption 5 (Potential outcome model). *For all $i \in \mathcal{N}$ $d \in \{0, 1\}$ and for all $g \in \mathcal{G}_i$*

$$Y_i(d, g) = m_{d,g}(X_i, \mathbf{X}_{S_i}) + \epsilon_{i,d,g} \quad (12)$$

with $\mathbb{E}[\epsilon_{i,d,g} | \mathbf{X}_n] = 0$, $\mathbf{X}_n = [X_1, \dots, X_n]$.

In this model, potential outcomes are functions of both X_i and \mathbf{X}_{S_i} , as well as other unobserved factors captured by the error term $\epsilon_{i,d,g}$. Under the extended SUTVA (Assumptions 1 and 2) the observed outcome is then given by

$$Y_i = m(X_i, \mathbf{X}_{S_i}) + \epsilon_i, \quad i = 1, \dots, n$$

where $m(X_i, \mathbf{X}_{S_i}) = \sum_{d,g} \mathbb{1}(D_i = d, G_i = g)m_{d,g}(X_i, \mathbf{X}_{S_i})$ and $\epsilon_i = \sum_{d,g} \mathbb{1}(D_i =$

$d, G_i = g) \epsilon_{i,d,g}$. Two sources of statistical dependence in outcomes across observations exist in this setting. First, the observed outcomes of different units are dependent through G_i because units can have overlapping interference sets. Second, network dependence may exist in the score variables and the error terms.

We assume that the data dependence structure can be described through *dependency neighborhoods*, determined by the network \mathbf{A} . Formally, a collection of random variables $\{Z_i\}_{i=1}^n$ has dependency neighborhoods $\mathbf{N}_i \subseteq \{1, \dots, n\}$, $i = 1, \dots, n$, if $i \in \mathbf{N}_i$, and Z_i is independent of $\{Z_j\}_{j \notin \mathbf{N}_i}$ (Ross, 2011, Definition 5.3). In other words, the dependency neighborhood of a unit i is a collection of indices of observations potentially dependent on observation i . We impose the following assumption:

Assumption 6 (Dependency neighborhoods). $\{(\{Y_i(d, g)\}_{d,g}, X_i, \mathbf{X}_{S_i}, D_i, G_i)\}_{i=1}^n$ has dependency neighborhoods $\mathbf{N}_i \subseteq \{1, \dots, n\}$, $i = 1, \dots, n$, where \mathbf{N}_i is a function of \mathbf{A} .

Letting $O_i = (Y_i, X_i, \mathbf{X}_{S_i}, D_i, G_i)$ be the observed data on unit i , it then holds that $\{O_i\}_{i=1}^n$ also has dependency neighborhoods \mathbf{N}_i , $i = 1, \dots, n$ under Assumption 6. Dependency neighborhoods can be represented by a *dependency graph* \mathbf{W} , a binary $n \times n$ matrix with entry $W_{ij} = 1$ if $j \in \mathbf{N}_i$ and $W_{ij} = 0$ otherwise. The dependency graph determines the amount of independent information available in the data. Indeed, by construction, for any two disjoint subsets $I_1, I_2 \subseteq \{1, \dots, n\}$ where $W_{ij} = 0$ for all $i \in I_1$ and $j \in I_2$ we have

$$\{O_i : i \in I_1\} \perp\!\!\!\perp \{O_j : j \in I_2\} \quad (13)$$

The results of the present section do not depend on the exact form of \mathbf{W} , but only on certain restrictions on its empirical degree distribution (see subsection 4.3). In practice, however, knowledge of \mathbf{W} is needed to perform inference. For example, two observations i and j can be dependent only if nodes i and j are at most two links apart in the network (second-order dependence) (e.g. Leung, 2020; Ogburn et al., 2022). In this case, we have $W_{ij} = \mathbb{1}(A_{ij} + \max_k A_{ik}A_{kj} + \mathbb{1}(i = j) > 0)$ as in Leung (2020). In general, the specific structure of \mathbf{W} will depend on the data-generating distribution and the assumed interference mechanism⁶.

⁶For instance, second-order dependence is consistent with network neighborhood interference

4.2 Distance-based estimator

We now introduce our distance-based estimation method for the boundary average causal effect $\tau_{d,g|d',g'}(\bar{\mathcal{X}}_{iS_i}(d,g|d',g'))$. The approach reduces the multivariate score (X_i, \mathbf{X}_{S_i}) to the normalized shortest Euclidean distance to the effective treatment boundary and performs a local polynomial estimation using this distance as the one-dimensional score (see Cattaneo et al., 2024, for a review).

Let $c = 0$ without loss generality and let $l_{d,g|d',g'}^{min}(X_i, \mathbf{X}_{S_i})$ be minimum Euclidean distance from $\bar{\mathcal{X}}_{iS_i}(d,g|d',g')$ of a random point (X_i, \mathbf{X}_{S_i}) . The minimum Euclidean distance is given by

$$X_{i,d,g,d',g'}^* = \mathbb{1}(D_i = d, G_i = g) \cdot l_{d,g|d',g'}^{min}(X_i, \mathbf{X}_{S_i}) - (1 - \mathbb{1}(D_i = d, G_i = g)) \cdot l_{d,g|d',g'}^{min}(X_i, \mathbf{X}_{S_i})$$

with realization $x_{i,d,g,d',g'}^*$. The distance-based linear local regression estimator is defined on the one-dimensional space of this distance variable $X_{i,d,g,d',g'}^*$.

For this purpose, let $T_i = \mathbb{1}(\mathbb{1}(D_i = d, G_i = g) + \mathbb{1}(D_i = d', G_i = g'))$ be the indicator variable taking value 1 if unit i belongs to either one of the two effective treatment regions $\mathcal{X}_{iS_i}(d, g)$ and $\mathcal{X}_{iS_i}(d', g')$ and 0 otherwise.

The estimation of the boundary average effects will not rely on the direct estimation of $m(X_i, \mathbf{X}_{S_i})$ but on the indirect estimation of a transformed model based on the distance transformation of (X_i, \mathbf{X}_{S_i}) . Let $\mu(X_{i,d,g,d',g'}^*) = \mathbb{E}[Y_i | X_{i,d,g,d',g'}^*, T_i = 1]$ be the expectation of the observed outcome conditional on the one-dimensional minimum Euclidean distance and on belonging to those effective treatment regions. Taking the expectation of model (12) with respect to $X_{i,d,g,d',g'}^*$ and T_i yields

$$Y_i = \mu(X_{i,d,g,d',g'}^*) + u_{i,d,g,d',g'}, \quad i = 1, \dots, n \quad (14)$$

where $u_{i,d,g,d',g'} = \nu_{i,d,g,d',g'} + \epsilon_i$ with $\nu_{i,d,g,d',g'} = m(X_i, \mathbf{X}_{S_i}) - \mu(X_{i,d,g,d',g'}^*)$. Note that we keep the assumption that $\mu(x_{i,d,g,d',g'}^*)$ is homogeneous across units. We relax this assumption in the Online Appendix A.

For convenience, let us denote $X_{i,d,g,d',g'}^*$ by X_i^* when it is not ambiguous, and let $\mu_{d,g}(0) = \lim_{x_i^* \downarrow 0} \mu(x_i^*)$ and $\mu_{d',g'}(0) = \lim_{x_i^* \uparrow 0} \mu(x_i^*)$. Here, the cutoff point $x_i^* = 0$

when the score variables are independently distributed and the error terms are exogenous and correlated up to second-order network neighbors.

represents the effective treatment boundary. The idea is to approximate in a flexible way the regression functions $\mu_{d,g}(x_i^*) = \mathbb{E}[Y_i(d, g) | X_i^* = x_i^*, T_i = 1]$ and $\mu_{d',g'}(x_i^*) = \mathbb{E}[Y_i(d', g') | X_i^* = x_i^*, T_i = 1]$ to the right and the left of $x_i^* = 0$ representing the effective treatment boundary, to estimate $\mu_{d,g}(0)$ and $\mu_{d',g'}(0)$. These quantities in turn approximate $\mathbb{E}[Y_i(d, g) | (X_i, \mathbf{X}_{S_i}) \in \bar{\mathcal{X}}_{iS_i}(d, g | d', g')]$ and $\mathbb{E}[Y_i(d', g') | (X_i, \mathbf{X}_{S_i}) \in \bar{\mathcal{X}}_{iS_i}(d, g | d', g')]$. Hence, our target estimand is $\tau_{d,g|d',g'}(0) = \mu_{d,g}(0) - \mu_{d',g'}(0)$. Assuming that the regression functions $\mu_{d,g}(x_i^*)$ and $\mu_{d',g'}(x_i^*)$ are at least twice differentiable at the cutoff, a first-order Taylor expansion of the functions around $x_i^* = 0$ yields

$$\begin{aligned}\mu_{d,g}(x_i^*) &\approx \mu_{d,g}(0) + \mu_{d,g}^{(1)}(0) \cdot x_i^* \\ \mu_{d',g'}(x_i^*) &\approx \mu_{d',g'}(0) + \mu_{d',g'}^{(1)}(0) \cdot x_i^*\end{aligned}\tag{15}$$

where $\mu_{d,g}^{(q)}(0)$ and $\mu_{d',g'}^{(q)}(0)$ denote the q^{th} derivative of $\mu_{d,g}(x_i^*)$ and $\mu_{d',g'}(x_i^*)$ in $x_i^* = 0$.

To simplify exposition, here we focus on a local linear estimator. However, in the Supplementary Material S.2 results are stated for polynomials with generic degree p . Setting $\beta_{d,g}(h_n) = [\beta_{d,g}^{(0)}, \beta_{d,g}^{(1)}]^T$ and $\beta_{d',g'}(h_n) = [\beta_{d',g'}^{(0)}, \beta_{d',g'}^{(1)}]^T$, the distance-based local linear estimators in this setting are obtained as

$$\begin{aligned}\hat{\beta}_{d,g}(h_n) &= \arg \min_{\beta_{d,g} \in \mathbb{R}^2} \sum_i \mathbb{1}(T_i = 1, X_i^* \geq 0) (Y_i - \beta_{d,g}^{(0)} - \beta_{d,g}^{(1)} X_i^*)^2 K_{h_n}(X_i^*) \\ \hat{\beta}_{d',g'}(h_n) &= \arg \min_{\beta_{d',g'} \in \mathbb{R}^2} \sum_i \mathbb{1}(T_i = 1, X_i^* < 0) (Y_i - \beta_{d',g'}^{(0)} - \beta_{d',g'}^{(1)} X_i^*)^2 K_{h_n}(X_i^*)\end{aligned}\tag{16}$$

where h_n is a positive bandwidth and $K_{h_n}(u) = K(u/h_n)/h_n$ for a given kernel function $K(\cdot)$. Then, $\hat{\beta}_{d,g}(h_n)$ and $\hat{\beta}_{d',g'}(h_n)$ are the estimators for $[\mu_{d,g}(0), \mu_{d,g}^{(1)}(0)]^T$ and $[\mu_{d',g'}(0), \mu_{d',g'}^{(1)}(0)]^T$. These estimators are obtained by fitting two separate linear regression models using kernel-weighted observations in each effective treatment region, and conditional on $T_i = 1$. We assume that the kernel function is a bounded, non-negative and symmetric function $K : [-1, 1] \rightarrow \mathbb{R}$ which is zero outside its support and integrates to 1, as is common in RDD literature (e.g., [Calonico et al., 2014](#))⁷.

We now introduce some useful notation, adapting the notation in [Calonico et al.](#)

⁷Commonly employed kernels include the uniform kernel, that assigns equal weight to each observation within the bandwidth, and the triangular kernel, which assigns weights that are monotonically decreasing with the distance from the cutoff point.

(2014). Let us set $\mathbf{Y} = [Y_1, \dots, Y_n]'$ and $\mathbf{X}_n^* = [X_1^*, \dots, X_n^*]^T$, and let $\mathbf{r}(u) = [1, u]$. We define $X^*(h_n) = [\mathbf{r}(X_1^*/h), \dots, \mathbf{r}(X_n^*/h)]$, that is, the matrix containing the linear expansion of the distance measure, the diagonal weighting matrices $W_{d,g}$ with generic diagonal element $w_{i,d,g} = \mathbb{1}(T_i = 1, X_i^* \geq 0) \cdot K_{h_n}(X_i^*)$, and $W_{d',g'}(h_n)$ with generic diagonal element $w_{i,d',g'} = \mathbb{1}(T_i = 1, X_i^* < 0) \cdot K_{h_n}(X_i^*)$. Finally, define $\Gamma_{d,g}(h_n) = X(h_n)'W_{d,g}(h_n)X(h_n)/n$ and $\Gamma_{d',g'}(h_n) = X(h_n)'W_{d',g'}(h_n)X(h_n)/n$. Letting $H = \text{diag}(1, h_n^{-1})$, for $h_n > 0$ the solutions to (16) are

$$\begin{aligned}\hat{\beta}_{d,g}(h_n) &= H(h_n)\Gamma_{d,g}^{-1}(h_n)X(h_n)^TW_{d,g}(h_n)\mathbf{Y}/n \\ \hat{\beta}_{d',g'}(h_n) &= H(h_n)\Gamma_{d',g'}^{-1}(h_n)X(h_n)^TW_{d',g'}(h_n)\mathbf{Y}/n\end{aligned}\tag{17}$$

The final estimator for $\hat{\tau}_{d,g|d',g'}$ is given by the difference in the estimators of the intercepts of the transformed outcome regression functions

$$\hat{\tau}_{d,g|d',g'}(h_n) = \hat{\mu}_{d,g}(h_n) - \hat{\mu}_{d',g'}(h_n)\tag{18}$$

where $\hat{\mu}_{d,g}(h_n) = e_1^T \hat{\beta}_{d,g}(h_n)$ and $\hat{\mu}_{d',g'}(h_n) = e_1^T \hat{\beta}_{d',g'}(h_n)$ with $e_1 = [1, 0]^T$.

4.3 Asymptotic Theory

We consider an asymptotic framework where $n \rightarrow \infty$. Because all causal estimands and estimators are conditioned on \mathbf{A} , our asymptotic framework assumes a sequence of networks \mathbf{A}_n , preserving fundamental aspects of the network topology as in [Ogburn et al. \(2022\)](#). The analysis of the asymptotic properties of $\hat{\tau}_{d,g|d',g'}(h_n)$ requires a constraint on the asymptotic growth of the dependence in the data.

We assume that certain moments of the (empirical) degree distribution of the dependency graph are asymptotically bounded so that the dependence in the observed data remains limited in scope.

Assumption 7 (Local Dependence). $n^{-1} \sum_i |\mathbf{N}_{i,n}|^3$ and $n^{-1} \sum_i \sum_{j \neq i} (\mathbf{W}_n^3)_{ij}$ are bounded.

This assumption is analogous to Assumption 4 in [Leung \(2020\)](#), although the dependency graphs are considered fixed in our case. The quantity $n^{-1} \sum_i |\mathbf{N}_{i,n}|^3$ is the empirical third moment of the degree distribution of \mathbf{W}_n whereas $n^{-1} \sum_{j \neq i} (\mathbf{W}_n^3)_{ij}$ is the average number of walks of length 3 emanating from unit i . These conditions

ensure that most units have a sufficiently small degree in the dependency graph with respect to the sample size while allowing degrees to increase with n . This guarantees a limited amount of dependence in the data as n becomes large.

For the proof of the asymptotic properties of $\hat{\tau}_{d,g|d',g'}(h_n)$, we follow [Masry and Fan \(1997\)](#) by focusing on the centered estimators (see Supplementary Material S.2). We consider $\hat{\tau}_{d,g,d',g'}^*(h_n) = e_1^T \hat{\beta}_{d,g}^*(h_n) - e_1^T \hat{\beta}_{d',g'}^*(h_n)$, obtained by replacing \mathbf{Y} with $\mathbf{u} = \mathbf{Y} - \mu(X^*)$ with $\mu(X^*) = [\mu(X_1^*), \dots, \mu(X_n^*)]$ in Equation (17). Under suitable smoothness assumptions on $\mu(X_i^*)$, some manipulation of a Taylor expansion of the centered estimator around the cutoff yields

$$\begin{aligned} \hat{\tau}_{d,g|d',g'}(h_n) - \tau_{d,g|d',g'}(0) &= \hat{\tau}_{d,g|d',g'}^*(h_n) + h_n^2 \left(\frac{\mu_{d,g}^{(2)}(0)}{2!} B_{d,g}(h_n) + \frac{\mu_{d',g'}^{(2)}(0)}{2!} B_{d',g'}(h_n) \right) \\ &\quad + T_{d,g,d',g'}(h_n) \end{aligned} \tag{19}$$

where $B_{d,g}(h_n) = \Gamma_{d,g}^{-1}(h_n) \theta_{d,g}(h_n)$ and $B_{d',g'}(h_n) = \Gamma_{d',g'}^{-1}(h_n) \theta_{d',g'}(h_n)$. Here, $\theta_{d,g}(h_n)$ and $\theta_{d',g',r}(h_n)$ are functions of the \mathbf{X}_n and the kernel weights, and $T_{d,g,d',g'}(h_n)$ is also a function of \mathbf{X}_n^* , the kernel weights and h_n and the Taylor remainder.

The proof proceeds in two main steps. The first step involves establishing the convergence of $\Gamma_{d,g}(h_n)$, $\Gamma_{d',g'}(h_n)$, $\theta_{d,g}(h_n)$ and $\theta_{d',g'}(h_n)$ to finite probability limits Γ and θ as $nh_n \rightarrow \infty$ and $h_n \rightarrow 0$. This is enabled by Assumption 7, which guarantees that their variances vanish asymptotically. Note also that under these assumptions $T_{d,g,d',g'}(h_n) = o_p(h^2)$. Convergence of the considered sample matrices then yields

$$(\hat{\tau}_{d,g|d',g'}(h_n) - \tau_{d,g,d',g'}(0)) = \hat{\tau}_{d,g|d',g'}^*(h_n) + h_n^2 B + o_p(h_n^2) \tag{20}$$

where $B = \frac{\mu_{d,g}^{(2)}(0) - \mu_{d',g'}^{(2)}(0)}{2!} e_1^T \Gamma^{-1} \theta$ and $\mu_{d,g}^{(2)}(0)$ and $\mu_{d',g'}^{(2)}(0)$ are the second derivative of $\mu(x_i^*)$ in $x_i^* = 0$.

Based on (20), the limiting distribution of $\sqrt{nh_n}(\hat{\tau}_{d,g|d',g'}(h_n) - \tau_{d,g,d',g'}(0))$ depends on the limiting distribution of $\sqrt{nh_n} \hat{\tau}_{d,g|d',g'}^*(h_n)$. Therefore, the second step establishes a central limit theorem for $\sqrt{nh_n} \hat{\tau}_{d,g|d',g'}^*(h_n)$ using Stein's method and leveraging the fact that replacing $\Gamma_{d,g}(h_n)$ and $\Gamma_{d',g'}(h_n)$ by Γ does not affect the limiting distribution of the centered estimator because of their consistency. Since we cannot condition on \mathbf{X}_n , this device effectively fixes the denominators $\Gamma_{d,g}(h_n)$ and $\Gamma_{d',g'}(h_n)$ ([Pagan and Ullah, 1999](#), page 115). Stein's method involves deriving

a bound on the distance between the estimator and a standard normal distribution. We leverage the bound derived in Theorem SA.4.1 in [Leung \(2020\)](#). This bound converges to zero under Assumption 7.

Both steps further rely on additional regularity conditions, which for brevity are detailed in the Supplementary Material S.2, Assumption S.2.1. These conditions include the convergence of the average distance density $n^{-1}f_i^*(x_i^*)$ to a bounded limit $\bar{f}^*(0)$, and the weighted average of conditional variances $n^{-1}\sum_i\sigma_{i,d,g}(x_i^*)f_i(x_i^*)$ and $n^{-1}\sum_i\sigma_{i,d',g'}(x_i^*)f_i(x_i^*)$ to bounded limits $\bar{\omega}_{d,g}(0)$ and $\bar{\omega}_{d',g'}(0)$. The asymptotic normality of $\hat{\tau}_{d,g|d',g'}(h_n)$ follows from (19), as given in the following theorem:

Theorem 4. *Suppose Assumption 7 and other smoothness and regularity conditions hold (Assumption S.2.1 - S.2.2 in Appendix S.2). If $nh_n \rightarrow \infty$, $h_n \rightarrow 0$ and $h_n = O(n^{1/2p+3})$, then*

$$\sqrt{nh_n}\left([\hat{\tau}_{d,g|d',g'}(h_n) - \tau_{d,g|d',g'}(0)] - h_n^2 e^T B\right) \xrightarrow{d} \mathcal{N}(0, V)$$

where

$$B = \frac{\mu_{d,g}^{(2)}(0) - \mu_{d',g'}^{(2)}(0)}{2!} e_1^T \Gamma^{-1} \theta, \quad V = \frac{\bar{\omega}_{d,g}(0) + \bar{\omega}_{d',g'}(0)}{\bar{f}^*(0)^2} e_1^T \Gamma^{-1} \Psi \Gamma^{-1} e_1 \quad (21)$$

The exact form of Γ , θ and Ψ is given in Supplementary Material S.2.

Proof. See Supplementary Material S.2..

Theorem 4 indicates that $\hat{\tau}_{d,g|d',g'}(h_n)$ converges to a normal distribution with asymptotic bias and variance given by $h_n^2 B$ and V/nh_n . The asymptotic bias depends on the second-order derivatives of the considered outcome regression functions, and it is not affected by \mathbf{W} . This is because the bias of local linear estimators depends essentially on the approximation error of the target functions. As a result, the conditional bias of $\hat{\tau}_{d,g|d',g'}(h_n)$ with dependent data aligns with the bias under independent data (see, e.g. [Calonico et al., 2014](#)). Additionally, the contribution of the leading bias to the asymptotic distribution of $\hat{\tau}_{d,g|d',g'}(h_n)$ can be removed by imposing the canonical condition $nh_n^5 \rightarrow 0$ ([Fan and Gijbels, 1996](#); [Calonico et al., 2014](#)).

The asymptotic variance is also unaffected by the data dependence structure. This is due to the local nature of the estimator combined with the sparseness entailed by Assumption 7. Indeed, for a fixed h_n we have that $nh_n \mathbb{V}[\tau_{d,g|d',g'}^*(h_n)] = \Psi_{d,g}(h_n) + \Psi_{d',g'}(h_n) - 2\Psi_{d,g,d',g'}(h_n)$, the sum of the variance of $e_1^T \beta_{d,g}^*(h_n)$ and

$e_1^T \beta_{d',g'}^*(h_n)$ minus double their covariance. The first two matrices incorporate the variance terms and the covariance terms of observations within the bandwidth to the right and the left of the cutoff, respectively. In contrast, the third matrix includes the covariance of observations across the cutoff. Such covariance terms vanish more quickly asymptotically because as the bandwidth shrinks to zero, the proportion of connected units within the bandwidth vanishes.

Therefore, under Assumption 7, the estimator $\hat{\tau}_{d,g|d',g'}(h_n)$ retains the same asymptotic distribution as under independent data. Similar results on the asymptotic distributional equivalence to the independent data case have been established of local linear estimators under different forms of data dependence, such as spatiotemporal dependence (Robinson, 1983; Masry and Fan, 1997; Opsomer et al., 2001; Robinson, 2011; Jenish, 2012). In the context of RDD, Bartalotti and Brummet (2017) find similar results in the case of clustered data with fixed size.

Remark 1. When a non-negligible fraction of units share the same nearest distance from the effective treatment boundary, due to common neighbors or shared score variables (e.g., family members with a common income index), the estimator $\hat{\tau}_{d,g|d',g'}(h_n)$ remains asymptotically normal. However, its asymptotic variance includes an additional term depending on the covariances of units sharing the same distance measure (see Lemma S.2.4 and Theorem S.2.4 in Supplementary Material S.2). In such cases, the joint density of the distance measure does not exist for these units, and the fraction of connected units within the bandwidth does not vanish asymptotically, breaking the equivalence to the independent data case.

Remark 2. The proposed estimator requires selecting a bandwidth h_n . The standard approach in RDDs for bandwidth selection minimizes the asymptotic Mean Squared Error (MSE) (Imbens and Kalyanaraman, 2012). Based on Theorem 4, the MSE-optimal bandwidth is $h_{n,opt} = \left(V/4B^2\right)^{\frac{1}{5}} n^{-\frac{1}{5}}$, for $B \neq 0$. The optimal bandwidth can be estimated using the plug-in selection procedure proposed by Calonico et al. (2014), which employs preliminary estimates of bias and variance with pilot bandwidths. Another possibility involves using plug-in estimators of the unknown quantities entering the asymptotic bias and variance (Imbens and Kalyanaraman, 2012).

4.4 Variance estimation

The results of the previous sections suggest that the use of standard variance estimators assuming independent data (e.g. [Calonico et al., 2014](#)) might be appropriate when n is large and h_n is small. However, the bandwidth h_n is never zero in finite samples, and the data dependence can affect the distribution of the estimator. Instead of directly estimating the asymptotic variance, we propose the following Eicker-Huber-White type estimator to account for such finite-sample dependence:

$$\hat{V}(h_n) = \hat{V}_{d,g}(h_n) + \hat{V}_{d',g'}(h_n) - 2\hat{C}_{d',g',d,g}(h_n) \quad (22)$$

where

$$\begin{aligned} \hat{V}_{d,g}(h_n) &= e_1^T \Gamma_{d,g}^{-1}(h_n) \hat{\Psi}_{d,g}(h_n) \Gamma_{d,g}^{-1}(h_n) e_1 / n \\ \hat{V}_{d',g'}(h_n) &= e_1^T \Gamma_{d',g'}^{-1}(h_n) \hat{\Psi}_{d',g'}(h_n) \Gamma_{d',g'}^{-1}(h_n) e_1 / n \\ \hat{C}_{d,g,d',g'}(h_n) &= e_1^T \Gamma_{d,g}^{-1}(h_n) \hat{\Psi}_{d,g,d',g'}(h_n) \Gamma_{d',g'}^{-1}(h_n) e_1 / n \end{aligned} \quad (23)$$

The estimators $\hat{\Psi}_{d,g}(h_n)$, $\hat{\Psi}_{d',g'}(h_n)$ and $\hat{\Psi}_{d,g,d',g'}(h_n)$ are given by

$$\begin{aligned} \hat{\Psi}_{d,g}(h_n) &= \mathcal{M}_{d,g}(h_n)^T \mathbf{W}_n \mathcal{M}_{d,g}(h_n) \\ \hat{\Psi}_{d',g'}(h_n) &= \mathcal{M}_{d',g'}(h_n)^T \mathbf{W}_n \mathcal{M}_{d',g'}(h_n) \\ \hat{\Psi}_{d,g,d',g'}(h_n) &= \mathcal{M}_{d,g}(h_n)^T \mathbf{W}_n \mathcal{M}_{d',g'}(h_n) \end{aligned} \quad (24)$$

In (24) \mathbf{W}_n is the dependency graph, and $\mathcal{M}_{d',g'}(h_n)$ and $\mathcal{M}_{d,g}(h_n)$ are $n \times 2$ matrices with i -th row given by the weighted linear expansion of X_i^*/h_n times the regression residual \hat{u}_i .

This variance estimator can be justified from a “fixed-bandwidth” perspective, which considers the estimator $\hat{\tau}_{d,g|d',g'}(h_n)$ as locally parametric holding the bandwidth fixed. In fact, the estimator in (22) estimates the fixed-bandwidth asymptotic variance of $\hat{\tau}_{d,g|d',g'}(h_n)$. The proposed estimator nests the case where $h_n \rightarrow 0$, and it is consistent for the asymptotic variance V/nh_n (see Theorem S.2.2 in Appendix S.2). Moreover, by indirectly estimating the asymptotic variance, it avoids estimating the unknown quantities $\bar{\omega}_+(0)$, $\bar{\omega}_-(0)$ and $\bar{f}^*(0)$ in V .

Similar arguments favoring Eicker-Huber-White type variance estimators can be found in [Chen et al. \(2014\)](#) in sieve inference for time series models, and [Kim et al. \(2017\)](#) in kernel-smoothing regression in time series. In RDDs with i.i.d. data,

Bartalotti (2019) demonstrates the robustness the EHW variance estimator to local heteroskedasticity.

4.5 Bias correction and robust confidence interval

In principle, as discussed in Section 4.3, the asymptotic bias of our RDD estimator $\hat{\tau}_{d,g|d',g'}(h_n)$ shown in Theorem 4 would go to zero if the canonical condition $nh_n^5 \rightarrow 0$ is met (Fan and Gijbels, 1996; Calonico et al., 2014). However, many common bandwidth selectors, including the MSE-optimal bandwidth, result in bandwidths that are too large to eliminate the leading bias contribution to the distributional approximation of the RDD estimator (Calonico et al., 2014). In RDD applications, it is then common to employ bias-corrected estimators. The standard method proposed by Calonico et al. (2014) recenters the RDD estimator by subtracting an estimate of the leading bias and rescales it with a variance estimator that accounts for the additional variability introduced by the bias-correction term. This approach yields confidence intervals that are robust to large bandwidths. We also consider bias correction in our setting.

Following Calonico et al. (2014), an estimator of the term B in Eq. (21) can be obtained by plugging in the local-quadratic estimators of the second derivatives $\frac{\mu_{d,g}^{(2)}(0)}{2!}$ and $\frac{\mu_{d',g'}^{(2)}(0)}{2!}$ using a bandwidth b_n . Let us denote this estimator as $\hat{B}(h_n, b_n)$. The bias-corrected estimator of $\tau_{d,g|d',g'}(\bar{\mathcal{X}}_{iS_i}(d, g | d', g'))$ is given by

$$\hat{\tau}_{d,g|d',g'}^{bc}(h_n, b_n) = \hat{\tau}_{d,g|d',g'}(h_n) - h_n^2 \hat{B}(h_n, b_n) \quad (25)$$

The estimator $\hat{\tau}_{d,g|d',g'}^{bc}(h_n, b_n)$ is asymptotically normal with zero mean and asymptotic variance coincident with the independent data case under the asymptotic regime of Calonico et al. (2014), (Theorem S.2.5, Supplementary Material S.2). This is not surprising given that $\hat{\tau}_{d,g|d',g'}^{bc}(h_n, b_n)$ differs from $\hat{\tau}_{d,g|d',g'}(h_n)$ by a term depending on local quadratic estimators, to which all previous considerations, *mutatis mutandis*, apply. Finally, the variance of $\hat{\tau}_{d,g|d',g'}^{bc}(h_n, b_n)$ can be estimated in a similar way as for $\hat{\tau}_{d,g|d',g'}(h_n)$, but with an extension to incorporate the additional variability induced by the bias correction term (see Supplementary Material S.2 for details).

4.6 Estimation of Boundary Overall Effect

The boundary overall direct effect $\tau_{1|0}$ is identified as the difference between the right and left limit of the observed outcome regression functions conditional on the individual score X_i as X_i approaches the cutoff under continuity assumptions (Theorem 3). We can rewrite the observed outcome model in (12) conditional on X_i as

$$\begin{aligned} Y_i &= \tilde{m}(X_i) + \nu_i + \epsilon_i \\ &= \tilde{m}(X_i) + u_i \end{aligned} \tag{26}$$

for $i = 1, \dots, n$, where $\tilde{m}(X_i) = \mathbb{E}[m(X_i, \mathbf{X}_{S_i}) | X_i]$, $\nu_i = m(X_i, \mathbf{X}_{S_i}) - \tilde{m}(X_i)$ and $u_i = \nu_i + \epsilon_i$.

Letting $c = 0$, Theorem 3 yields

$$\begin{aligned} \tau_{1|0} &= \lim_{x_i \downarrow 0} \mathbb{E}[Y_i | X_i = x_i] - \lim_{x_i \uparrow 0} \mathbb{E}[Y_i | X_i = x_i] \\ &= \lim_{x_i \downarrow 0} \tilde{m}(x_i) - \lim_{x_i \uparrow 0} \tilde{m}(x_i) \end{aligned}$$

A natural choice is to estimate the limits $\tilde{m}_1(0) = \lim_{x_i \downarrow 0} \tilde{m}(x_i)$ and $\tilde{m}_0(0) = \lim_{x_i \uparrow 0} \tilde{m}(x_i)$ by local linear regression using the individual score variable as the univariate regressor and without considering \mathbf{X}_{S_i} , as in the standard no-interference RDD. To do so, we solve

$$\begin{aligned} \hat{\beta}_1(h_n) &= \arg \min_{\beta_1 \in \mathbb{R}^2} \sum_i \mathbb{1}(X_i \geq 0) (Y_i - \beta_1^{(0)} - \beta_1^{(1)} X_i)^2 K_{h_n}(X_i), \\ \hat{\beta}_0(h_n) &= \arg \min_{\beta_0 \in \mathbb{R}^2} \sum_i \mathbb{1}(X_i < 0) (Y_i - \beta_0^{(0)} - \beta_0^{(1)} X_i)^2 K_{h_n}(X_i), \end{aligned}$$

The final estimator of $\tau_{1|0}$ is given by

$$\hat{\tau}_{1|0}(h_n) = e_1^T \hat{\beta}_1(h_n) - e_1^T \hat{\beta}_0(h_n) \tag{27}$$

Consistency and asymptotic normality of $\hat{\tau}_{1|0}(h_n)$ are established in Supplementary Material S.2. The asymptotic distribution of $\hat{\tau}_{1|0}(h_n)$ matches that under independent data, with a bias depending on the second-order derivatives of $\tilde{m}(X_i)$ ⁸.

⁸In Supplementary Material S.2, proofs are stated for the generic RDD p -order local polynomial

A variance estimator can be constructed analogously to estimator 24, replacing the distance measure with X_i and using the corresponding regression residual. This estimator accounts for dependence among observations on each side and across the cutoff using the dependency graph. Furthermore, the difference between this estimator and the typical RDD heteroskedasticity-robust variance estimator (Calonico et al., 2014) increases with the level of dependence in the data. When \mathbf{W} is diagonal (independent data), these estimators coincide.

5 Simulation study

In this section, we report the results of a simulation study demonstrating the finite-sample properties of $\hat{\tau}_{1|0}(h_n)$ and $\hat{\tau}_{d,g|d',g'}(h_n)$, and their bias-corrected version $\hat{\tau}_{1|0}^{bc}(h_n, b_n)$ and $\hat{\tau}_{d,g|d',g'}^{bc}(h_n, b_n)$.

In this exercise, units are clustered in groups of size 3, that is, \mathbf{A} is a block diagonal matrix with blocks of dimension 3×3 blocks. Let $\{1z, 2z, 3z\}$ be the set of units in group z , for $z = 1, \dots, Z$. Interference occurs within groups so that $\mathcal{S}_{iz} = \{jz, kz\}$, where jz and kz denote the neighbors of the generic unit i in group z , with $j, k \in \{1, 2, 3\} \neq i$. We use the one treated exposure mapping, i.e., $G_i = \mathbb{1}\{D_{jz} + D_{kz} > 0\}$

We simulate data from the model:

$$Y_{iz} = m(X_{iz}, \mathbf{X}_{\mathcal{S}_{iz}}) + \epsilon_{iz}$$

where

$$m(x_{iz}, \mathbf{x}_{\mathcal{S}_{iz}}) = \begin{cases} 7.2 + 3.2x_{iz} + 7.2x_{iz}^2 + 3.3x_{jz} + 1.2x_{kz} + 0.2x_{jz}x_{kz}, & \text{if } D_{iz} = 1, G_{iz} = 0 \\ 6.7 + 2.9x_{iz} + 3.2x_{iz}^2 + 4.3x_{jz} + 0.8x_{kz} + 0.2x_{jz}x_{kz}, & \text{if } D_{iz} = 1, G_{iz} = 1 \\ 0.9 + 1.7x_{iz} - 1.5x_{iz}^2 + 3.3x_{jz} + 1.2x_{kz} + 0.2x_{jz}x_{kz}, & \text{if } D_{iz} = 0, G_{iz} = 0 \\ 3.5 + 1.2x_{iz} - 3.1x_{iz}^2 + 4.3x_{jz} + 0.8x_{kz} + 0.2x_{jz}x_{kz}, & \text{if } D_{iz} = 0, G_{iz} = 1 \end{cases}$$

These outcome regression functions are non-linear in individual and neighborhood scores, so the proposed estimators may exhibit some bias without the bias correction.

estimator for $\tau_{1|0}$, for ease of exposition. Results for $\hat{\tau}_{d,g|d',g'}(h_n)$ follow by analogy.

Additionally, causal effects vary across different points of the treatment boundaries.

We generate the score variables such that are independent across groups and correlated within groups. In each group, z , $(X_{1z}, X_{2z}, X_{3z})^T$ are simulated from a truncated multivariate normal, with zero mean vector and variance-covariance

$$\Sigma = \begin{bmatrix} 1 & 0.5 & 0.8 \\ 0.5 & 1 & 0.8 \\ 0.8 & 0.8 & 1 \end{bmatrix}$$

with upper and lower bound equal to -5 and 5 for each component of $(X_{1z}, X_{2z}, X_{3z})^T$.

For the error terms, we simulate a vector $\eta = (\eta_{1z}, \eta_{2z}, \eta_{3z})^T$ of exogenous i.i.d. variables, with $\eta_{iz} \sim \mathcal{N}(0, 1)$, and for $jz \in \mathcal{S}_{iz}$ $\tilde{\eta}_{jz} = \eta_{jz}[2 \cdot \mathbb{1}(D_{iz} + D_{jz} = 2) + 4 \cdot \mathbb{1}(D_{iz} + D_{jz} = 0) - 2 \cdot \mathbb{1}(D_{iz} + D_{jz} = 1)]$. The final error term is given by $\epsilon_{iz} = \frac{1}{2}(\tilde{\eta}_{jz} + \tilde{\eta}_{kz}) + \eta_{iz}$, so that the correlation between the error terms of two neighbors is heterogeneous depending on whether they score below, above, or on different sides of the cutoff.

In this scenario, each unit's score space is partitioned into four treatment regions and the potential outcome regression functions are non-linear functions of the individual and neighborhood scores. Furthermore, observations are correlated within each cluster but not across clusters, so the dependency graph is given by a binary block-diagonal matrix with blocks of dimension 3×3 .

We simulate 1000 datasets with increasing sample size $N = \{750, 1500, 3000, 6000\}$ and increasing number of groups $Z = \{250, 300, 1000, 2000\}$. For each dataset, we estimate the boundary overall direct effect using the estimator in (27), the boundary direct effects $\tau_{10|00}(\mathcal{X}_{is_i}(10|00))$ and $\tau_{11|01}(\mathcal{X}_{is_i}(11|01))$, and the boundary indirect effects $\tau_{01|00}(\mathcal{X}_{is_i}(01|00))$ and $\tau_{11|10}(\mathcal{X}_{is_i}(11|10))$, using the estimator defined in Eq. (18) (Table 1). In addition, for sample size $N = 3000$, we also estimate the same causal effects using the bias-corrected estimators defined in Eq. 25 (Table 2).

Table 1 presents the results for the estimators without bias correction. Columns "S.D." and "S.E." report the empirical standard deviation and the average estimated standard error using the variance estimator defined in Eq. (22). Column S.E.*.i.i.d.* displays the average estimated standard error using the heteroskedasticity-robust plug-in residuals variance estimator without weights from the `rdrubust` package [Calonico et al. \(2017\)](#). The purpose of including this variance estimator is to evaluate its

performance, given that it assumes i.i.d. data, and the data dependence should be asymptotically irrelevant. Columns “C.R.” and “C.R.*i.i.d.*” shows the coverage rate corresponding to S.E. and S.E.*i.i.d.*, respectively. Lastly, columns “ $N_{d,g}$ ” and “ $N_{d',g'}$ ” indicate the average sample size within the bandwidth on each side of the effective treatment boundary. We estimate a different bandwidth for each sample size and effect following the procedure in [Calonico et al. \(2014\)](#), although all estimators are indexed by h_n for convenience.

Several considerations emerge from this simulation exercise. First, the boundary direct effects estimators, $\hat{\tau}_{10|00}(h_n)$ and $\hat{\tau}_{11|01}(h_n)$, show a slow decrease in bias with increasing sample size, unlike the indirect effects estimators, $\hat{\tau}_{01|00}(h_n)$ and $\hat{\tau}_{11|10}(h_n)$, which exhibit minimal bias. This discrepancy arises from the differing degrees of non-linearity in the target outcome regression functions conditional on the minimum distance measure. Specifically, the outcome regression functions for the boundary direct effects are non-linear, whereas those for the boundary indirect effects are approximately linear near the effective treatment boundary. Second, our variance estimator generally yields more accurate estimates of the empirical standard deviation than the i.i.d. variance estimator across different effects and sample sizes. The level of improvement depends on the clustering induced by the treatment assignment. The improvement is more substantial for the boundary indirect effect estimator $\hat{\tau}_{01|00}(h_n)$, due to the presence of a relevant average fraction of units with common minimum distance measure $\bar{\mathcal{X}}_{iS_i}(01|00)$, which induces further clustering at the minimum distance measure level. Third, the empirical standard errors for the boundary indirect effects estimators are generally higher than those for direct effects estimators, likely due to greater heterogeneity of the point indirect effects on the effective treatment boundary. Lastly, as the sample size increases, the coverage rates for $\hat{\tau}_{01|00}(h_n)$ and $\hat{\tau}_{11|10}(h_n)$ approach the nominal rate, while those for $\hat{\tau}_{10|00}(h_n)$ and $\hat{\tau}_{11|01}(h_n)$ do not improve, due to the selected bandwidth that fail to fully remove the contribution of the leading bias to the distribution of the estimators.

		Bias	SD	S.E.	S.E. _{<i>i.i.d.</i>}	CR	CR _{<i>i.i.d.</i>}	$\bar{N}_{d,g}$	$\bar{N}_{d',g'}$
N = 750	$\hat{\tau}_{1 0}(h_n)$	-0.265	1.487	1.358	1.293	0.93	0.91	143.58	191.92
	$\hat{\tau}_{10 00}(h_n)$	-0.154	2.860	2.319	2.254	0.890	0.883	30.761	54.154
	$\hat{\tau}_{11 01}(h_n)$	-0.184	1.798	1.603	1.547	0.929	0.924	81.526	73.928
	$\hat{\tau}_{01 00}(h_n)$	0.007	3.079	2.572	1.996	0.906	0.813	84.709	123.631
	$\hat{\tau}_{11 10}(h_n)$	-0.027	3.803	2.865	2.827	0.889	0.886	42.533	29.676
N = 1500	$\hat{\tau}_{1 0}(h_n)$	-0.247	1.037	0.968	0.921	0.930	0.912	286.417	381.773
	$\hat{\tau}_{10 00}(h_n)$	-0.138	1.927	1.620	1.577	0.905	0.892	64.539	116.677
	$\hat{\tau}_{11 01}(h_n)$	-0.099	1.256	1.147	1.103	0.936	0.927	164.575	149.318
	$\hat{\tau}_{01 00}(h_n)$	0.009	2.025	1.798	1.391	0.935	0.846	177.135	262.354
	$\hat{\tau}_{11 10}(h_n)$	-0.002	2.331	2.026	1.997	0.910	0.909	90.311	61.249
N = 3000	$\hat{\tau}_{1 0}(h_n)$	-0.242	0.772	0.698	0.664	0.896	0.879	560.023	739.773
	$\hat{\tau}_{10 00}(h_n)$	-0.141	1.272	1.135	1.098	0.920	0.913	134.619	250.087
	$\hat{\tau}_{11 01}(h_n)$	-0.157	0.906	0.818	0.785	0.924	0.911	326.281	297.351
	$\hat{\tau}_{01 00}(h_n)$	0.000	1.419	1.274	0.979	0.931	0.838	361.820	540.826
	$\hat{\tau}_{11 10}(h_n)$	0.058	1.695	1.450	1.426	0.913	0.907	186.916	126.535
N = 6000	$\hat{\tau}_{1 0}(h_n)$	-0.233	0.568	0.507	0.484	0.891	0.874	1066.788	1386.329
	$\hat{\tau}_{10 00}(h_n)$	-0.131	0.894	0.806	0.778	0.934	0.922	268.927	498.379
	$\hat{\tau}_{11 01}(h_n)$	-0.158	0.640	0.591	0.568	0.923	0.916	629.096	574.371
	$\hat{\tau}_{01 00}(h_n)$	0.021	0.994	0.886	0.680	0.925	0.825	735.370	1109.016
	$\hat{\tau}_{11 10}(h_n)$	0.034	1.145	1.024	1.006	0.939	0.934	382.333	255.386

Table 1: Simulation results with groups of size three and one treated exposure mapping. One thousand replications. S.D. = empirical standard error. S.E. = estimated standard error. S.E._{*i.i.d.*} = estimated standard error with *i.i.d.* heteroskedasticity-robust HC0 plug-in residuals variance estimator. C.R. = coverage rate. C.R._{*i.i.d.*} = coverage rate corresponding to the *i.i.d.* heteroskedasticity-robust HC0 plug-in residuals variance estimator. $\bar{N}_{d,g}$ and $\bar{N}_{d',g'}$ = effective sample size on each side of the treatment boundary.

Table 2 presents the results for the bias-corrected versions of the considered estimators. The estimators for the boundary direct effects effectively remove the leading bias from the estimate. In addition, the estimated confidence intervals also provide better coverage of the true values across effects, reaching a rate close to the nominal level. Here, our standard error estimator and the *i.i.d.* estimator perform similarly, with the largest difference observed in the estimation of the standard error of $\hat{\tau}_{01|00}(h_n)$. Overall, the empirical standard errors are greater than those in Table 1 due to the additional variability introduced by the bias correction term.

		Bias	SD	S.E.	S.E. _{<i>i.i.d.</i>}	CR	CR _{<i>i.i.d.</i>}	$\tilde{N}_{d,g}$	$\tilde{N}_{d',g'}$
N = 3000	$\hat{\tau}_{1 0}^{bc}(h_n, b_n)$	-0.06	0.82	0.79	0.76	0.94	0.93	561.89	744.77
	$\hat{\tau}_{10 00}^{bc}(h_n, b_n)$	-0.05	1.45	1.33	1.30	0.94	0.92	134.07	249.55
	$\hat{\tau}_{11 01}^{bc}(h_n, b_n)$	0.03	1.01	0.94	0.91	0.94	0.93	327.90	298.36
	$\hat{\tau}_{01 00}^{bc}(h_n, b_n)$	0.08	1.60	1.50	1.16	0.94	0.86	361.35	542.01
	$\hat{\tau}_{11 10}^{bc}(h_n, b_n)$	-0.04	1.89	1.72	1.70	0.95	0.95	188.09	126.91

Table 2: Simulation results using bias correction with groups of size three and one treated exposure mapping. One thousand replications. S.D. = empirical standard error. S.E. = estimated standard error. S.E._{*i.i.d.*} = estimated standard error with *i.i.d.* heteroskedasticity-robust HC0 plug-in residuals variance estimator. C.R. = coverage rate. C.R._{*i.i.d.*} = coverage rate corresponding to the *i.i.d.* heteroskedasticity-robust HC0 plug-in residuals variance estimator. $N_{d,g}$ and $N_{d',g'}$ = effective sample size on each side of the treatment boundary.

Additional simulation studies are presented in Appendix B, where we evaluate our estimation method under more complex scenarios, including varying group sizes and network structures.

6 Empirical Illustration

PROGRESA, later renamed Oportunidades and finally, Prospera was a governmental social assistance program initiated in Mexico in 1997. The program targeted poverty by providing cash transfers to poor households, conditional upon children’s regular school attendance and health clinic visits.

In the program’s initial phase, 506 villages from seven rural states in Mexico were selected. Among these, 320 villages were randomly assigned to the treatment group, while the remaining 186 villages served as the control group. In the subsequent phase, households within the treatment villages were selected to receive the subsidy based on a household poverty index.

Several studies have highlighted the success of PROGRESA in enhancing educational outcomes (Skoufias and Parker, 2009). Moreover, the spillover effects generated by the program have been examined using linear-in-means models by Bobonis and Finan (2009) and Lalive and Cattaneo (2009), leveraging the initial randomization. Arduini et al. (2020) further incorporated heterogeneous externalities into their analysis. Here, we focus on the second phase of the program, and examine exclusively data from the 320 villages where households were selected to receive cash transfers.

The data consist of repeated observations for 24,000 households over three consecutive academic years (1997-1998, 1998-1999, and 1999-2000), with each academic year starting in August and ending in June. Baseline characteristics were collected in October 1997, while subsidies began in August 1998. The first wave of post-treatment data was collected in October 1998, and a second post-treatment survey was conducted in November 1999.

The score variable is the centered household poverty index used to determine program eligibility, and the outcome is school enrollment in academic year 1998-1999. We use our proposed method to estimate the direct and indirect effects of eligibility to the program for children whose household poverty index and whose friends' household poverty index positioned them on the effective treatment boundaries.

We select children from treatment villages who live with their mothers, for whom we have completed school enrollment data for 1997 and 1998, and who had completed grades 3 to 6 by October 1997, similar to [Lalive and Cattaneo \(2009\)](#). However, we only include those children who were enrolled in school for the 1997-1998 academic year, as they are more likely to have interacted in the village school during that academic year. Moreover, we focus exclusively on villages in regions 3 (Sierra Negra-Zongolica-Mazateca), 4 (Sierra Norte-Otomi Tepehua), and 5 (Sierra Gorda), where the cutoff values were nearly identical to avoid pooling observations with different cutoff values ([Cattaneo et al., 2016](#)).

We define clusters based on village, completed grade in October 1997 and gender, as within a village homophily in friendship networks among children is especially strong along these dimensions (see e.g., [Shrum et al., 1988](#)). For valid inference, it is necessary to assume stable friendship links among children over time. This assumption is supported by the program's timing, the absence of evidence for relocation across villages between 1997 and 1998, and the enrollment in school for the year 1997-1998 for all the children in our sample.

Our final sample consists of 5,174 observations with unequally-sized interference sets. We restrict the analysis on children who have at most three neighbors, which makes the assumption of homogeneous outcome expectations more plausible (see the Online Appendix A for a discussion on this assumption). This reduces the sample to 3,111 observations. For this empirical exercise, we define the exposure mapping as the fraction of treated units in the interference set: $G_i = \frac{\sum_{j \in \mathcal{S}_i} D_j}{|\mathcal{S}_i|}$. We estimate the direct effect of the eligibility to the cash transfer on school enrolment in the academic year

1998-1999 when having neighbors all eligible ($G_i = 1$) and when having neighbors all ineligible ($G_i = 0$). Additionally, we estimate the spillover effect of having all eligible neighbors ($G_i = 1$) compared to having all ineligible neighbors ($G_i = 0$) on school attendance for someone eligible or ineligible. Finally, we estimate the boundary overall direct effect of being eligible for the cash transfer⁹.

The effective treatment boundary corresponding to our estimands are described in Table 3 along with the range of the computed minimum distance measure and number of observations on each effective treatment region.

	Boundary	All observations		Treatment		Control	
		N	Range	N	Range	N	Range
$\tau_{1 0}$	$X_i = 0, X_j \in \mathbb{R} \forall j \in \mathcal{S}_i$	5174	[-542.50, 467.00]	3316	[0.00, 467.00]	1858	[-542.50, -0.10]
$\tau_{10 00}(\bar{\mathcal{X}}_{i\mathcal{S}_i}(10 00))$	$X_i = 0, X_j < 0 \forall j \in \mathcal{S}_i$	597	[-527.75, 365.50]	233	[0.00, 365.50]	364	[-527.75, -0.50]
$\tau_{11 01}(\bar{\mathcal{X}}_{i\mathcal{S}_i}(11 01))$	$X_i = 0, X_j \geq 0 \forall j \in \mathcal{S}_i$	1303	[-542.50, 379.50]	957	[0.50, 379.50]	346	[-542.50, -0.50]
$\tau_{01 00}(\bar{\mathcal{X}}_{i\mathcal{S}_i}(01 00))$	$X_i < 0, X_j = 0 \forall j \in \mathcal{S}_i$	710	[-700.72, 478.44]	346	[0.00, 478.44]	364	[-700.72, -0.50]
$\tau_{11 10}(\bar{\mathcal{X}}_{i\mathcal{S}_i}(11 10))$	$X_i \geq 0, X_j = 0 \forall j \in \mathcal{S}_i$	1190	[-542.50, 575.94]	957	[0.50, 575.94]	233	[-542.50, -0.50]

Table 3: Boundaries and sample sizes of each effect for PROGRESA data. The range refers to the individual score variable in the first line and the minimum distance score in the remaining lines.

Table 4 reports the estimates using our proposed estimators. Standard errors and confidence intervals are computed using the variance estimator described in subsection 4.4. The estimates with and without bias correction are similar and are therefore discussed jointly.

The boundary overall direct effect is positive, indicating a significant marginal impact of eligibility to PROGRESA on children’s school enrollment. The boundary direct effect for children with ineligible neighbors is also positive and significant, while the direct effect when having eligible neighbors is smaller and non-significant. Estimates for the boundary indirect effects suggest that the impact of having all eligible neighbors versus all ineligible neighbors is greater for ineligible children than for eligible children. However, the standard error is large in both cases, resulting in confidence intervals with lower negative bounds. Overall, these results suggest that the program benefits school attendance, mostly directly for children with ineligible peers.

⁹Here, we maintain the assumption of homogeneous individual boundary effects. This assumption may be justifiable as we focus on small, similarly sized interference sets.

The varying magnitudes of the estimated effects can be attributed to their local nature. For example, a lower poverty index correlates with better living conditions and more educated parents (Lalive and Cattaneo, 2009). Children with non-poor friends, who are more likely to attend school, may be more encouraged to attend school upon receiving a subsidy, explaining the larger estimate of $\hat{\tau}_{10|00}(h_n)$ compared to $\hat{\tau}_{11|01}(h_n)$.

The estimator $\hat{\tau}_{01|00}(h_n)$ and $\hat{\tau}_{11|10}(h_n)$ estimate a spillover effect on ineligible (non-poor) and eligible (poor) children, respectively, whose friends have a poverty index near the cutoff. A non-poor family may find it easier to send their child to school when their child's friends attend school because of the subsidy, as they face less economic burden. On the other hand, children from low-income families might face a negative incentive when their friends are eligible and thus attend school more frequently. For instance, if fewer children work, wages might increase, incentivizing poor children to seek employment over education (Attanasio et al., 2011).

	Estimate	S.E.	95% C.I.	p-value	$N_{d,g}$	$N_{d',g'}$
$\hat{\tau}_{1 0}(h_n)$	0.076	0.032	(0.014, 0.138)	0.017	741	1010
$\hat{\tau}_{1 0}^{bc}(h_n, b_n)$	0.072	0.036	(0.001, 0.143)	0.046	741	1010
$\hat{\tau}_{10 00}(h_n)$	0.238	0.071	(0.098, 0.377)	0.001	202	129
$\hat{\tau}_{10 00}^{bc}(h_n, b_n)$	0.263	0.080	(0.106, 0.420)	0.001	202	129
$\hat{\tau}_{11 01}(h_n)$	0.024	0.044	(-0.063, 0.111)	0.587	216	325
$\hat{\tau}_{11 01}^{bc}(h_n, b_n)$	0.012	0.050	(-0.086, 0.109)	0.816	216	325
$\hat{\tau}_{01 00}(h_n)$	0.077	0.098	(-0.116, 0.269)	0.434	170	158
$\hat{\tau}_{01 00}^{bc}(h_n, b_n)$	0.097	0.120	(-0.139, 0.332)	0.421	170	158
$\hat{\tau}_{11 10}(h_n)$	-0.046	0.043	(-0.131, 0.038)	0.282	158	353
$\hat{\tau}_{11 10}^{bc}(h_n, b_n)$	-0.050	0.052	(-0.152, 0.052)	0.333	158	353

Table 4: Estimates for PROGRESA data with conventional and robust confidence intervals, MSE-optimal bandwidths.

S.E. = estimated standard errors, C.I. = Normal approximation confidence intervals. p-value = Normal approximation two-sided p-value. $N_{d,g}$, $N_{d',g'}$ = Effective sample sizes

7 Conclusions

In this paper, we have provided an analytical framework for interference in the continuity-based approach to RDDs. Here, potential outcomes are influenced by the treatment of units within interference sets through an exposure mapping. We have shown that the non-probabilistic nature of the individual treatment assignment results in a non-probabilistic assignment of the effective treatment, allowing us to interpret RDDs under interference as multiscore RDDs. In this context, the effective treatment depends on both individual scores and the scores of units in the interference set. We have characterized the resulting multiscore space in terms of effective treatment regions and boundaries and introduced novel causal estimands. We have identified such effects through generalized continuity assumptions. An important finding is that the overall direct effect at the cutoff is identified as the difference in the right and left limit of the outcome conditional expectation at the cutoff point, which coincides with the identification strategy in the no-interference RDDs.

We have proposed a distance-based local polynomial estimator for estimating boundary effects and the standard RDD local polynomial estimator for estimating the boundary overall direct effect. We have considered these estimation strategies with and without bias correction, and have derived their asymptotic properties under an assumption of local dependence. To our knowledge, this is the first work to consider local polynomial estimation with network-dependent data, thus indirectly contributing to the statistical literature on local polynomial estimators (Fan and Gijbels, 1996). We have validated the properties of our proposed estimators in an extensive simulation study. Finally, we have illustrated our method to estimate boundary direct and indirect effects of Progesa on children’s school attendance.

Our framework does have some limitations, which also present opportunities for future research. We assume that the network is fixed and fully observed without error, and that the exposure mapping is correctly specified. However, accurate network information might be unavailable, and the “true” exposure mapping could be unknown. Misspecifying the network and exposure mapping entails the misspecification of the multiscore space. Exploring this possibility would be worthwhile.

In the case of non-compliance to treatment eligibility/assignment (fuzzy RDD), we have focused on intention-to-treat effects. Identifying the average effect of treatment receipt for compliers requires additional assumptions (Imbens and Lemieux,

2008; Dong, 2018; Arai et al., 2022). Under interference, non-compliance adds several complexities (Imai et al., 2021; DiTraglia et al., 2023). In addition, generalizing identifying monotonicity assumptions from univariate to multivariate settings has proven challenging in RDDs (Choi and Lee, 2023). However, our formalization of interference might offer a foundation for exploring these complex scenarios.

Our distance-based estimators performed well in our simulations, but they may have drawbacks. For instance, distance-based estimators may behave poorly in high-dimensional data (Aggarwal et al., 2001). Furthermore, this method relies on a data transformation that might not be optimal because it groups all observations with the same distance from the boundary to the same point in the unidimensional distance space, potentially increasing bias (Imbens and Wager, 2019). Existing literature on multiscore RDDs has predominantly concentrated on simpler scenarios featuring bivariate scores and two treatment regions. However, interference in large groups or dense networks may lead to high-dimensional and unequally-sized boundaries. Therefore, another direction for future research is developing alternative non-parametric estimation methods to handle this new setting effectively.

Supplementary Material

In Supplementary Material S.1 we provide the proofs of Theorem 1, 2 and 3. In Supplementary Material S.2 we detail the asymptotic theory for the estimators in Section 4. The Supplementary Material is available upon request.

References

- Aggarwal, C. C., Hinneburg, A., and Keim, D. A. (2001). On the surprising behavior of distance metrics in high dimensional spaces. In *International Conference on Database Theory*.
- Angelucci, M. and De Giorgi, G. (2009). Indirect effects of an aid program: How do cash transfers affect ineligibles' consumption? *American Economic Review*, 99(1):486–508.
- Arai, Y., Hsu, Y.-C., Kitagawa, T., Mourifié, I., and Wan, Y. (2022). Testing identifying assumptions in fuzzy regression discontinuity designs. *Quantitative Economics*, 13(1):1–28.
- Arduini, T., Patacchini, E., and Rainone, E. (2020). Treatment effects with heterogeneous externalities. *Journal of Business & Economic Statistics*, 38(4):826–838.
- Aronow, P. M., Basta, N. E., and Halloran, M. E. (2017). The regression discontinuity design under interference: A local randomization-based approach. *Observational Studies*, 3(2).
- Aronow, P. M. and Samii, C. (2017). Estimating average causal effects under general interference, with application to a social network experiment. *The Annals of Applied Statistics*, 11(4):1912–1947.
- Athey, S., Eckles, D., and Imbens, G. (2015). Exact p-values for network interference. *NBER Working Paper 21313*.
- Attanasio, O. P., Meghir, C., and Santiago, A. (2011). Education choices in mexico: Using a structural model and a randomized experiment to evaluate progresá. *The Review of Economic Studies*, 79(1):37–66.
- Baird, S., Bohren, J. A., McIntosh, C., and Özler, B. (2018). Optimal design of experiments in the presence of interference. *The Review of Economics and Statistics*, 100(5):844–860.
- Bartalotti, O. (2019). Regression discontinuity and heteroskedasticity robust standard errors: Evidence from a fixed-bandwidth approximation. *Journal of Econometric Methods*, 8(1):20160007.

- Bartalotti, O. and Brummet, Q. (2017). Regression discontinuity designs with clustered data. In *Regression Discontinuity Designs*, volume 38, pages 383–420. Emerald Group Publishing Limited.
- Black, S. E. (1999). Do better schools matter? parental valuation of elementary education. *Quarterly Journal of Economics*, 114(2):577–99.
- Bobonis, G. J. and Finan, F. (2009). Neighborhood peer effects in secondary school enrollment decision. *The Review of Economics and Statistics*, 91(4):695–716.
- Bowers, J., Fredrickson, M., and Panagopoulos, C. (2013). Reasoning about interference between units: a general framework. *Political Analysis*, 21(1):97–124.
- Calonico, S., Cattaneo, M., Farrell, M. H., and Titiunik, R. (2017). rdrobust: Software for regression-discontinuity designs. *Stata Journal*, 17(2):372–404.
- Calonico, S., Cattaneo, M. D., Farrell, M. H., and Titiunik, R. (2019). Regression Discontinuity Designs Using Covariates. *The Review of Economics and Statistics*, 101(3):442–451.
- Calonico, S., Cattaneo, M. D., and Titiunik, R. (2014). Robust nonparametric confidence intervals for regression-discontinuity designs. *Econometrica*, 82(6):2295–2326.
- Cattaneo, M. D., Idrobo, N., and Titiunik, R. (2024). *A Practical Introduction to Regression Discontinuity Designs: Extensions*. Cambridge University Press.
- Cattaneo, M. D., Keele, L., Titiunik, R., and Vazquez-Bare, G. (2016). Interpreting regression discontinuity designs with multiple cutoffs. *The Journal of Politics*, 78(4):1229–1248.
- Chen, X., Liao, Z., and Sun, Y. (2014). Sieve inference on possibly misspecified semi-nonparametric time series models. *Journal of Econometrics*, 178(P3):639–658.
- Choi, J. and Lee, M. (2023). Complier and monotonicity for fuzzy multi-score regression discontinuity with partial effects. *Economics Letters*, 228:111169.
- Christakis, N. and Fowler, J. (2009). *Connected: The Surprising Power of Our Social Networks and How They Shape Our Lives*. Little, Brown.
- Cox, D. R. (1958). *Planning of Experiments*. New York: Wiley.

- Dell, M. (2010). The persistent effects of peru’s mining ”mita”. *Econometrica*, 78(6):1863–1903.
- DiTraglia, F. J., García-Jimeno, C., O’Keeffe-O’Donovan, R., and Sánchez-Becerra, A. (2023). Identifying causal effects in experiments with spillovers and non-compliance. *Journal of Econometrics*, 235(2):1589–1624.
- Dong, Y. (2018). Alternative assumptions to identify late in fuzzy regression discontinuity designs. *Oxford Bulletin of Economics and Statistics*, 80(5):1020–1027.
- Emmenegger, C., Spohn, M., and Bühlmann, P. (2022). Treatment effect estimation from observational network data using augmented inverse probability weighting and machine learning.
- Fan, J. and Gijbels, I. (1996). *Local Polynomial Modelling and Its Applications*. Chapman and Hall, London.
- Forastiere, L., Airoidi, E. M., and Mealli, F. (2021). Identification and estimation of treatment and interference effects in observational studies on networks. *Journal of the American Statistical Association*, 116(534):901–918.
- Forastiere, L., Mealli, F., Wu, A., and Airoidi, E. M. (2022). Estimating causal effects under network interference with bayesian generalized propensity scores. *Journal of Machine Learning Research*, 23(289):1–61.
- Halloran, M. E. and Struchiner, C. J. (1995). Causal inference in infectious diseases. *Epidemiology*, 6(2):142–151.
- Hanh, J., Todd, P., and van der Klaauw, W. (2001). Identification and estimation of treatment effects with a regression-discontinuity design. *Econometrica*, 69(1):201–09.
- Hernan, M. and Robins, J. (2023). *Causal Inference: What If*. CRC Press, 1st ed. edition.
- Hong, G. and Raudenbush, S. W. (2006). Evaluating kindergarten retention policy: A case study of causal inference for multilevel observational data. *Journal of the American Statistical Association*, 101:901–910.

- Hudgens, M. G. and Halloran, M. E. (2008). Toward causal inference with interference. *Journal of the American Statistical Association*, 103(482):832–842.
- Imai, K., Jiang, Z., and Malani, A. (2021). Causal inference with interference and noncompliance in two-stage randomized experiments. *Journal of the American Statistical Association*, 116(534):632–644.
- Imbens, G. and Kalyanaraman, K. (2012). Optimal bandwidth choice for the regression discontinuity estimator. *The Review of Economic Studies*, 79(3):933–959.
- Imbens, G. and Lemieux, T. (2008). Regression discontinuity designs: A guide to practice. *Journal of Econometrics*, 142(2):615–35.
- Imbens, G. and Wager, S. (2019). Optimized regression discontinuity designs. *The Review of Economics and Statistics*, 101(2):264–278.
- Imbens, G. and Zajonc, T. (2011). Regression discontinuity design with multiple forcing variables. Working Paper.
- Jackson, M. O. (2008). *Social and economic networks*. Princeton University Press.
- Jenish, N. (2012). Nonparametric spatial regression under near-epoch dependence. *Journal of Econometrics*, 167(1):224–239.
- Keele, L. J. and Titiunik, R. (2015). Geographic boundaries as regression discontinuities. *Political Analysis*, 23(1):127–155.
- Kim, M. S., Sun, Y., and Yang, J. (2017). A fixed-bandwidth view of the pre-asymptotic inference for kernel smoothing with time series data. *Journal of Econometrics*, 197(2):298–322.
- Kojevnikov, D., Marmer, V., and Song, K. (2021). Limit theorems for network dependent random variables. *Journal of Econometrics*, 222(2):882–908.
- Kolesár, M. and Rothe, C. (2018). Inference in regression discontinuity designs with a discrete running variable. *American Economic Review*, 108(8):2277–2304.
- Lalive, R. and Cattaneo, M. A. (2009). Social interactions and schooling decisions. *The Review of Economics and Statistics*, 91(3):457–477.

- Lee, D. S. (2008). Randomized experiments from non-random selection in u.s. house elections. *Journal of Econometrics*, 142(2):675–97.
- Lee, D. S. and Card, D. (2008). Regression discontinuity inference with specification error. *Journal of Econometrics*, 142(2):655–674.
- Leung, M. (2020). Treatment and spillover effects under network interference. *The Review of Economics and Statistics*, 102(2):368–380.
- Leung, M. P. and Loupos, P. (2023). Unconfoundedness with network interference.
- Liu, L. and Hudgens, M. (2014). Large sample randomization inference of causal effects in the presence of interference. *Journal of the American Statistical Association*, 109(505):288–301.
- Liu, L., Hudgens, M. G., and Becker-Dreps, S. (2016). On inverse probability-weighted estimators in the presence of interference. *Biometrika*, 103.
- Manski, C. F. (2013). Identification of treatment response with social interactions. *The Econometrics Journal*, 16(1):S1–S23.
- Masry, E. and Fan, J. (1997). Local polynomial estimation of regression functions for mixing processes. *Scandinavian Journal of Statistics*, 24(2):165–179.
- Matsudaira, J. D. (2008). Mandatory summer school and student achievement. *Journal of Econometrics*, 142(2):829–850.
- McPherson, M., Smith-Lovin, L., and Cook, J. M. (2001). Birds of a feather: Homophily in social networks. *Annual Review of Sociology*, 27(1):415–444.
- Ogburn, E. and VanderWeele, T. (2017). Vaccines, contagion, and social networks. *Annals of Applied Statistics*, 11:919–948.
- Ogburn, E. L., Sofrygin, O., Díaz, I., and van der Laan, M. J. (2022). Causal inference for social network data. *Journal of the American Statistical Association*, 0(0):1–15.
- Opsomer, J., Wang, Y., and Yang, Y. (2001). Nonparametric regression with correlated errors. *Statistical Science*, 16(2):134–53.
- Pagan, A. and Ullah, A. (1999). *Nonparametric Econometrics*. Themes in Modern Econometrics. Cambridge University Press.

- Papadogeorgou, G., Mealli, F., and CM, Z. (2019). Causal inference with interfering units for cluster and population level treatment allocation programs. *Biometrics*, 75(3):778–787.
- Perez-Heydrich, C., Hudgens, M. G., Halloran, M. E., Clemens, J. D., Ali, M., and Emch, M. E. (2014). Assessing effects of cholera vaccination in the presence of interference. *Biometrics*, 70:731–744.
- Reardon, S. F. and Robinson, J. P. (2012). Regression discontinuity designs with multiple rating-score variables. *Journal of Research on Educational Effectiveness*, 5(1):83–104.
- Robinson, P. (2011). Asymptotic theory for nonparametric regression with spatial data. *Journal of Econometrics*, 165(1):5–19.
- Robinson, P. M. (1983). Nonparametric estimators for time series. *Journal of Time Series Analysis*, 4(3):185–207.
- Ross, N. (2011). Fundamentals of stein’s method. *Probability Surveys*, 8(none):210–293.
- Rubin, D. B. (1986). Which ifs have causal answers? comment on “statistics and causal inference” by p. holland. *Journal of the American Statistical Association*, 81.
- Shrum, W., Cheek, N. H., and Hunter, S. M. (1988). Friendship in school: Gender and racial homophily. *Sociology of Education*, 61(4):227–239.
- Skoufias, E. and Parker, S. (2009). *The Impact of PROGRESA on Child Labor and Schooling*, pages 167–185. Palgrave Macmillan US.
- Sobel, M. E. (2006). What do randomized studies of housing mobility demonstrate? *Journal of the American Statistical Association*, 101(476):1398–1407.
- Sofrygin, O. and van der Laan, M. (2017). Semi-parametric estimation and inference for the mean outcome of the single time-point intervention in a causally connected population. *Journal of Causal Inference*, 5.
- Tchetgen Tchetgen, E. J. and VanderWeele, T. J. (2012). On causal inference in the presence of interference. *Statistical Methods in Medical Research*, 21:55–75.

- Trochim, W. (1984). *Research Design for Program Evaluation: The Regression-Discontinuity Approach*. Contemporary Evaluation Research Series. Sage Publications, Beverly Hills, Calif.
- van der Laan, M. J. (2014). Causal inference for a population of causally connected units. *Journal of Causal Inference*, 2(1):13–74.
- Wong, V. C., Steiner, P. M., and Cook, T. D. (2013). Analyzing regression-discontinuity designs with multiple assignment variables: A comparative study of four estimation methods. *Journal of Educational and Behavioral Statistics*, 38(2):107–141.

Online Appendix to “Regression Discontinuity Designs Under Interference”

A Heterogeneous effects

This section extends the analysis to scenarios where units can have different outcome conditional expectations and scores distribution. In general, both the outcomes and score distributions may depend on the characteristics of the observed network. For example, this may occur when units have varying numbers of neighbors, potentially leading to heterogeneous (conditional) outcome expectations (Emmenegger et al., 2022; Ogburn et al., 2022). In this case the dimension of the multiscore space, and thus the joint score density $f(x_i, \mathbf{x}_{S_i})$, also varies across units.

When the conditional outcome expectations are heterogeneous, the estimands of interest are defined as the average of such expectations across the network nodes.

Let $\mathcal{N}_s = \{i \in \mathcal{N} : |\mathcal{S}_i| = s\}$ be the set of all units having exactly s neighbors. We redefine the boundary point causal effects as

$$\tau_{s,d,g|d',g'}(\bar{x}_i, \bar{\mathbf{x}}_{S_i}) = \frac{1}{|\mathcal{N}_s|} \sum_{i \in \mathcal{N}_s} \mathbb{E}_i[Y_i(d, g) - Y_i(d', g') \mid (X_i, \mathbf{X}_{S_i}) = (\bar{x}_i, \bar{\mathbf{x}}_{S_i})] \quad (\text{A.1})$$

The definition of N_s is necessary with unequally-sized interference, as boundary point effects can only be defined for subsets of units with the same number of neighbors. This is because these effects are dimension-specific: by conditioning on (X_i, \mathbf{X}_{S_i}) , they also condition on the dimension of the interference set (and the multiscore space).

In contrast, boundary causal effects can be defined for the entire sample as follows

$$\tau_{d,g|d',g'}(\bar{\mathcal{X}}_{iS_i}(d, g | d', g')) = \frac{1}{N} \sum_i \tau_{i,d,g,d',g'}(\bar{\mathcal{X}}_{iS_i}(d, g | d', g')) \quad (\text{A.2})$$

where $\tau_{i,d,g,d',g'}(\bar{\mathcal{X}}_{iS_i}(d, g | d', g')) = \mathbb{E}_i[Y_i(d, g) - Y_i(d', g') | (X_i, \mathbf{X}_{S_i}) \in \bar{\mathcal{X}}_{iS_i}(d, g | d', g')]$ represents the unit-specific expected difference in potential outcomes at their effective treatment boundary, which have potentially different dimensions.

Lastly, the boundary overall direct effect is defined as

$$\tau_{1|0} = \frac{1}{N} \sum_i \sum_{g \in \mathcal{G}_i} \tau_{i,1,g|0,g}(\bar{\mathcal{X}}_{iS_i}(1, g | 0, g)) \cdot \mathbb{P}_i(G_i = g | X_i = c) \quad (\text{A.3})$$

i.e., the average of unit-specific boundary overall direct effects.

Identification of the boundary point and boundary average causal effects is achieved under Assumption 4. Specifically, if the continuity of the outcome regression functions and score densities, as well as the other regularity conditions, hold for every unit, it follows that

$$\begin{aligned} \tau_{s,d,g|d',g'}(\bar{x}_i, \bar{\mathbf{x}}_{S_i}) &= \frac{1}{|\mathcal{N}_s|} \sum_{i \in \mathcal{N}_s} \lim_{\epsilon \rightarrow 0} \mathbb{E}_i[Y_i | (X_i, \mathbf{X}_{S_i}) \in \mathcal{B}_{\epsilon,d,g|d',g'}^{d,g}(\bar{x}_i, \bar{\mathbf{x}}_{S_i})] \\ &\quad - \lim_{\epsilon \rightarrow 0} \mathbb{E}_i[Y_i | (X_i, \mathbf{X}_{S_i}) \in \mathcal{B}_{\epsilon,d,g|d',g'}^{d',g'}(\bar{x}_i, \bar{\mathbf{x}}_{S_i})] \end{aligned}$$

and

$$\begin{aligned} \tau_{d,g|d',g'}(\bar{\mathcal{X}}_{iS_i}(d, g | d', g')) &= \frac{1}{N} \sum_i \lim_{\epsilon \rightarrow 0} \mathbb{E}_i[Y_i | (X_i, \mathbf{X}_{S_i}) \in \mathcal{B}_{\epsilon,d,g|d',g'}^{d,g}(\bar{x}_i, \bar{\mathbf{x}}_{S_i})] \\ &\quad - \lim_{\epsilon \rightarrow 0} \mathbb{E}_i[Y_i | (X_i, \mathbf{X}_{S_i}) \in \mathcal{B}_{\epsilon,d,g|d',g'}^{d',g'}(\bar{x}_i, \bar{\mathbf{x}}_{S_i})] \end{aligned}$$

by analogous arguments as in Theorem 2. Finally, identification of the boundary overall direct effect is given by

$$\tau_{1|0} = \frac{1}{N} \sum_i \lim_{x_i \downarrow c} \mathbb{E}_i[Y_i | X_i = x_i] - \lim_{x_i \uparrow c} \mathbb{E}_i[Y_i | X_i = x_i]$$

Turning to estimation, in section 4 we derived the analytical properties of a nonparametric estimator for the boundary average causal effect and overall direct effect under the assumption of homogeneity in the target outcome regression func-

tions. However, if these functions differ across units, due to heterogeneous conditional outcome expectations, our estimation strategy no longer estimates the estimands defined in (A.2) and (A.3). Instead, it consistently estimates a weighted average of unit-specific conditional expectations, with weights depending on the score marginal densities.

To clarify this point, let us consider the estimation of the overall direct effect using the estimator in subsection 4.6, and suppose that the observed outcomes models is

$$Y_i = \tilde{m}_i(X_i) + \epsilon_i$$

where $\tilde{m}_i(X_i)$ is now i -specific. Suppose further that the boundary overall direct effect $\tau_{1|0}$ defined in (A.3) has a finite limit as n becomes large. The cutoff is $c = 0$. Finally, let $\tau_{i,1|0} = \sum_{g \in \mathcal{G}_i} \tau_{i,1,g|0,g}(\bar{\mathcal{X}}_{iS_i}(1, g | 0, g) \cdot \mathbb{P}(G_i = g | X_i = c))$. Then it is possible to show that under our assumptions in Theorem S.2.1

$$\hat{\tau}_{1|0}(h_n) \xrightarrow{p} \lim_{n \rightarrow \infty} \frac{\sum_i (\tilde{m}_{i,1}(0) - \tilde{m}_{i,0}(0)) \cdot f_i(0)}{\sum_i f_i(0)} \quad (\text{A.4})$$

where $\tilde{m}_{i,1}(0) = \lim_{x_i \downarrow 0} \tilde{m}(x_i)$, $\tilde{m}_{i,0}(0) = \lim_{x_i \uparrow 0} \tilde{m}(x_i)$ and $f_i(x_i)$ is the individual score marginal density, which is also i -specific. Under Assumption 4 the RHS of (A.4) corresponds to the weighted average of unit-specific overall direct effects, weighted by their relative individual score densities at the cutoff. Finally, it is worth noting that the heterogeneity discussed in this section can also arise from other fixed attributes, in addition to the network. In this case, the outcome expectations are also conditioned on such fixed attributes and the arguments of the present section apply.

B Additional Simulation Results

B.1 Network Data

In this subsection, we propose a simulation study where we evaluate the performance of the bias-corrected estimators $\hat{\tau}_{1|0}^{bc}(h_n, b_n)$ and $\hat{\tau}_{d,g|d',g'}^{bc}(h_n, b_n)$ when data are characterized by irregular data structures, i.e., non-overlapping groups with different group sizes or network data with overlapping interference sets.

The purpose of this simulation study is to evaluate the finite-sample properties and the asymptotic properties of $\hat{\tau}_{1|0}^{bc}(h_n, b_n)$ and $\hat{\tau}_{d,g|d',g'}^{bc}(h_n, b_n)$ when interference sets

are also irregular because they are defined based on the underlying data structure.

In this simulation study, for each unit the interference set contains only linked units, and G_i is given by the one treated exposure mapping. We consider two scenarios.

Scenario A: Units belong to groups of size 2 to 6 (\mathbf{A} is block-diagonal with blocks of varying size). We simulate 1000 datasets with an increasing number of groups, specifically $\{50, 100, 200, 400\}$, for each group size. This results in datasets with sample sizes $N = \{300, 750, 1500, 3000, 6000\}$. The average number of neighbors is 3 in every dataset.

Scenario B: units are connected through a network. We simulate 1000 datasets with sample size $N = \{300, 750, 1500, 3000, 6000\}$, and for each sample size, we generate a network where links are formed at random with a bounded maximal degree, $K_{max} = 5$. The average degree is approximately 3.

Outcomes are simulated according from the following model

$$Y_i = 0.5 + D_i + 0.5X_i + 0.2\bar{\mathbf{X}}_{\mathcal{S}_i} + 0.7G_i - 0.4D_iG_i + \epsilon_i \quad (\text{B.1})$$

where X_i is independently and identically distributed as a truncated normal with mean 0 and variance 1, and upper and lower bound -5 and 5. The error term is given by $\epsilon_i = \frac{\sum_{j \in \mathcal{S}_i} \xi_j}{|\mathcal{S}_i|}$ with $\xi_i \stackrel{i.i.d.}{\sim} \mathcal{N}(0, 1)$. $\bar{\mathbf{X}}_{\mathcal{S}_i}$ is the average of the scores of units in \mathcal{S}_i . Therefore, in scenario A observations are independent across groups and the dependency graph is also block-diagonal. In scenario B, observations are dependent up to second-order network neighbors (second-order dependence). Note that in this simulation study boundary average effects do not depend on the network and are homogeneous across units.

Results of the simulation study are reported in Table B.1 (Scenario A) and B.2 (Scenario B). The tables report the empirical bias, empirical standard deviation, estimated standard error using our proposed variance estimator, and the estimated confidence interval coverage rate. Additionally, they provide the average effective sample sizes (columns $N_{d,g}$ and $N_{d',g'}$) and the percentage of units with unique score variables and minimum distance measures (column “Common”). A value less than 1 in this column signals the presence of shared distance measures. We select the bandwidth for each estimator using the procedure described in [Calonico et al. \(2014\)](#).

According to the results in Table B.1, our estimators show slight bias in small samples ($N = 300$ and $N = 750$), with bias decreasing as the sample size increases. The standard deviation of the estimators also decreases substantially in large samples. Notably, $\hat{\tau}_{1|0}^{bc}(h_n, b_n)$ has a lower standard deviation compared to other estimators due to the larger average effective sample size, whereas the standard deviation of $\hat{\tau}_{10|00}(h_n, b_n)$ is the largest due to small effective sample size. This is due to the low average fraction of units with $(D_i = 1, G_i = 0)$.

We highlight, however, that the standard deviation of $\hat{\tau}_{01|00}(h_n, b_n)$ is significantly high despite the relatively large average effective sample size for each N . This is due to the substantial clustering induced by the distance transformation. Only 49% of the observations have distinct distance measures, meaning that 61% of units share the same distance measure with at least one other unit. This clustering, artificially induced by the distance measure transformation, occurs because units in clusters necessarily have the same neighbors.

A comparison with the estimated standard error reveals that our standard error estimators are unbiased for the true standard deviation in large samples ($N = 3000, N = 6000$), where also the coverage rates reach the nominal rate.

Similar conclusions can be drawn from the results in Table B.2, showing results from scenario B. The bias and standard deviation are comparable to those in Table B.1 for most estimators. However, here the standard deviation of $\hat{\tau}_{01|00}(h_n, b_n)$ is significantly lower due to the reduced clustering induced by the distance transformation, as the simulated networks are sparser compared to scenario A.

Scenario A

		Bias	S.D.	S.E.	C.R.	$N_{d,g}$	$N_{d',g'}$	Common
N = 750	$\hat{\tau}_{1 0}^{bc}(h_n, b_n)$	0.00	0.53	0.50	0.93	125.82	172.82	1.00
	$\hat{\tau}_{10 00}^{bc}(h_n, b_n)$	0.05	1.01	0.88	0.91	45.14	60.68	1.00
	$\hat{\tau}_{11 01}^{bc}(h_n, b_n)$	0.00	0.66	0.60	0.93	76.97	105.51	1.00
	$\hat{\tau}_{01 00}^{bc}(h_n, b_n)$	0.03	0.91	0.79	0.92	138.00	108.82	0.49
	$\hat{\tau}_{11 10}^{bc}(h_n, b_n)$	0.01	0.88	0.81	0.94	56.76	45.35	0.94
N = 1500	$\hat{\tau}_{1 0}^{bc}(h_n, b_n)$	0.01	0.36	0.35	0.95	257.66	357.34	1.00
	$\hat{\tau}_{10 00}^{bc}(h_n, b_n)$	0.02	0.66	0.62	0.93	93.56	128.50	1.00
	$\hat{\tau}_{11 01}^{bc}(h_n, b_n)$	0.03	0.45	0.42	0.94	158.99	220.20	1.00
	$\hat{\tau}_{01 00}^{bc}(h_n, b_n)$	0.01	0.60	0.57	0.94	284.89	224.46	0.49
	$\hat{\tau}_{11 10}^{bc}(h_n, b_n)$	0.04	0.62	0.57	0.93	118.91	94.46	0.94
N = 3000	$\hat{\tau}_{1 0}^{bc}(h_n, b_n)$	-0.02	0.26	0.25	0.94	523.66	730.06	1.00
	$\hat{\tau}_{10 00}^{bc}(h_n, b_n)$	-0.03	0.48	0.44	0.94	192.18	264.55	1.00
	$\hat{\tau}_{11 01}^{bc}(h_n, b_n)$	0.01	0.31	0.30	0.94	323.89	451.24	1.00
	$\hat{\tau}_{01 00}^{bc}(h_n, b_n)$	-0.02	0.43	0.40	0.94	584.83	456.14	0.49
	$\hat{\tau}_{11 10}^{bc}(h_n, b_n)$	0.02	0.41	0.40	0.94	246.87	195.52	0.93
N = 6000	$\hat{\tau}_{1 0}^{bc}(h_n, b_n)$	-0.03	0.19	0.17	0.95	1064.38	1492.69	1.00
	$\hat{\tau}_{10 00}^{bc}(h_n, b_n)$	-0.03	0.32	0.31	0.94	392.06	546.17	1.00
	$\hat{\tau}_{11 01}^{bc}(h_n, b_n)$	-0.01	0.22	0.21	0.94	658.62	919.81	1.00
	$\hat{\tau}_{01 00}^{bc}(h_n, b_n)$	-0.03	0.29	0.28	0.95	1207.54	935.90	0.49
	$\hat{\tau}_{11 10}^{bc}(h_n, b_n)$	-0.02	0.30	0.28	0.93	503.76	395.00	0.93

Table B.1: Simulation results for Scenario A over one thousand replications. S.D. = empirical standard error. S.E. = estimated standard error. C.R. = coverage rate. $N_{d,g}$ and $N_{d',g'}$ = effective sample size on each side of the treatment boundary.

Scenario B

		Bias	S.D.	S.E.	C.R.	N _{d,g}	N _{d',g'}	Common
N = 750	$\hat{\tau}_{1 0}^{bc}(h_n, b_n)$	0.01	0.56	0.49	0.93	134.80	185.04	1.00
	$\hat{\tau}_{10 00}^{bc}(h_n, b_n)$	0.04	0.99	0.87	0.92	47.96	64.64	1.00
	$\hat{\tau}_{11 01}^{bc}(h_n, b_n)$	0.00	0.68	0.57	0.91	82.34	112.55	1.00
	$\hat{\tau}_{01 00}^{bc}(h_n, b_n)$	0.04	0.62	0.56	0.94	146.89	113.11	0.80
	$\hat{\tau}_{11 10}^{bc}(h_n, b_n)$	0.00	0.90	0.81	0.92	62.23	48.60	0.90
N = 1500	$\hat{\tau}_{1 0}^{bc}(h_n, b_n)$	0.01	0.36	0.34	0.94	278.00	386.82	1.00
	$\hat{\tau}_{10 00}^{bc}(h_n, b_n)$	0.01	0.64	0.61	0.95	100.72	138.42	1.00
	$\hat{\tau}_{11 01}^{bc}(h_n, b_n)$	0.01	0.44	0.40	0.94	169.86	234.62	1.00
	$\hat{\tau}_{01 00}^{bc}(h_n, b_n)$	-0.01	0.44	0.40	0.93	302.23	232.08	0.81
	$\hat{\tau}_{11 10}^{bc}(h_n, b_n)$	0.00	0.60	0.57	0.94	129.29	99.57	0.90
N = 3000	$\hat{\tau}_{1 0}^{bc}(h_n, b_n)$	-0.01	0.25	0.24	0.95	560.80	781.60	1.00
	$\hat{\tau}_{10 00}^{bc}(h_n, b_n)$	-0.01	0.45	0.43	0.94	207.20	286.01	1.00
	$\hat{\tau}_{11 01}^{bc}(h_n, b_n)$	0.00	0.30	0.28	0.94	342.88	474.84	1.00
	$\hat{\tau}_{01 00}^{bc}(h_n, b_n)$	0.00	0.29	0.28	0.95	616.74	470.52	0.81
	$\hat{\tau}_{11 10}^{bc}(h_n, b_n)$	0.00	0.41	0.40	0.95	266.83	206.14	0.90
N = 6000	$\hat{\tau}_{1 0}^{bc}(h_n, b_n)$	0.00	0.17	0.17	0.95	1142.75	1602.55	1.00
	$\hat{\tau}_{10 00}^{bc}(h_n, b_n)$	0.00	0.33	0.30	0.94	415.17	575.00	1.00
	$\hat{\tau}_{11 01}^{bc}(h_n, b_n)$	0.00	0.20	0.20	0.95	707.56	989.75	1.00
	$\hat{\tau}_{01 00}^{bc}(h_n, b_n)$	0.00	0.20	0.20	0.96	1260.84	946.53	0.81
	$\hat{\tau}_{11 10}^{bc}(h_n, b_n)$	0.01	0.30	0.28	0.94	549.78	414.41	0.90

Table B.2: Simulation results for Scenario B over one thousand replications. S.D. = empirical standard error. S.E. = estimated standard error. C.R. = coverage rate. N_{d,g} and N_{d',g'} = effective sample size on each side of the treatment boundary.

B.2 Varying group size

In the following simulation study, data are clustered in equally-sized groups, indexed by $z = 1, \dots, Z$. We consider two scenarios. In the first scenario, we keep the group size N_z fixed and vary Z . In the second scenario, we keep the sample size N fixed and we increase Z so that N_z decreases. The main purpose is to evaluate the performance of our proposed estimators with bias correction when treatment boundaries have a higher dimension than in the main text simulation 5.

Scenario A We simulate 1000 datasets with group size $N_z = \{3, 4, 5, 6, 8\}$ and

fixed number of groups $Z = 1000$, with corresponding sample size increases $N = \{3000, 4000, 5000, 6000, 8000\}$.

Scenario B We simulate 1000 datasets with group size $N_z = \{3, 4, 5, 6, 8\}$ and fixed sample size $N = 3000$, with corresponding number of groups $Z = \{1000, 750, 600, 500, 375\}$.

Data are simulated as in the previous subsection. In each scenario, we consider, for brevity, $\hat{\tau}_{1|0}^{bc}(h_n, b_n)$, $\hat{\tau}_{10|00}^{bc}(h_n, b_n)$, and $\hat{\tau}_{01|00}^{bc}(h_n, b_n)$ ¹.

The results for Scenario A are reported in Table B.3, while the results for Scenario B are presented in Table B.4.

From Table B.3, several observations emerge. $\hat{\tau}_{1|0}^{bc}(h_n, b_n)$ is unbiased in each scenario with an empirical standard error that decreases as the group and sample size increase.

$\hat{\tau}_{10|00}^{bc}(h_n, b_n)$, and $\hat{\tau}_{01|00}^{bc}(h_n, b_n)$ are mostly unbiased for $N_z = \{3, 4, 5, 6\}$, but their bias slightly increases for $N_z = 8$. For both estimators, the empirical standard error is lower in the scenario with $N_z = 4$ compared to other groups sizes, but it is higher when $N_z = \{6, 8\}$. This is likely due to the reduction in the effective sample size despite a larger overall sample size N , as increasing groups sizes correspond to higher-dimensional effective treatment boundaries and sparser observations around these boundaries.

The increase in the empirical standard error is more marked for $\hat{\tau}_{01|00}^{bc}(h_n, b_n)$, possibly due to the clusterization in the space of the distance measure, as can be deduced from column “Shared distance.” Indeed, for $N_z = 8$, only 19% observations have distinct distance measures. As for the standard error estimators, we observe a worsening in performance for the estimator of the standard error of $\hat{\tau}_{10|00}^{bc}(h_n, b_n)$, and $\hat{\tau}_{01|00}^{bc}(h_n, b_n)$ as the cluster size increases, with consequent deterioration of the coverage rate, unlike $\hat{\tau}_{1|0}^{bc}(h_n, b_n)$.

These results suggest that our proposed estimation method for the boundary average causal effect is mostly effective when the group size is moderate. When the group size is large, and thus the effective treatment boundaries are high-dimensional, a substantial sample size is required to compensate for the above-mentioned issues.

¹The bandwidth h_n and b_n are computed using the recursive procedure proposed by [Calonico et al. \(2014\)](#).

However, the performance of the boundary overall direct effect estimator remains similar across different group sizes.

The results in Table B.4 also supports these observations. As expected, all considered estimators compared to Table B.3 have higher standard errors for $N_z \geq 4$, due to the smaller sample size. The increase in the empirical standard error compared to Table B.3, is especially marked for $\hat{\tau}_{10|00}^{bc}(h_n, b_n)$, and $\hat{\tau}_{01|00}^{bc}(h_n, b_n)$, and the small sample size exacerbates the poor performance of the variance estimator.

Finally, we highlight that despite these issues, the bias remains moderate in all scenarios, likely due to the effect homogeneity along the effective treatment boundaries. We speculate that with heterogeneous effects, the increased dimension of the treatment boundaries might also lead to increased bias.

Scenario A - Fixed number of groups $Z = 1000$

	Bias	S.D.	S.E.	C.R.	$N_{d,g}$	$N_{d',g'}$	Common	
$N_z = 3$	$\hat{\tau}_{1 0}^{bc}(h_n, b_n)$	0.00	0.27	0.25	0.94	560.42	780.39	1.00
	$\hat{\tau}_{10 00}^{bc}(h_n, b_n)$	0.00	0.40	0.37	0.93	262.22	361.62	1.00
	$\hat{\tau}_{01 00}^{bc}(h_n, b_n)$	0.00	0.41	0.38	0.93	545.68	548.76	0.63
$N_z = 4$	$\hat{\tau}_{1 0}^{bc}(h_n, b_n)$	-0.01	0.19	0.19	0.95	756.25	1059.52	1.00
	$\hat{\tau}_{10 00}^{bc}(h_n, b_n)$	0.01	0.36	0.34	0.94	243.09	335.36	1.00
	$\hat{\tau}_{01 00}^{bc}(h_n, b_n)$	0.00	0.41	0.38	0.94	689.08	552.08	0.44
$N_z = 5$	$\hat{\tau}_{1 0}^{bc}(h_n, b_n)$	0.01	0.17	0.16	0.95	951.93	1332.39	1.00
	$\hat{\tau}_{10 00}^{bc}(h_n, b_n)$	0.01	0.36	0.34	0.93	209.22	289.46	1.00
	$\hat{\tau}_{01 00}^{bc}(h_n, b_n)$	0.01	0.43	0.40	0.93	715.11	496.22	0.33
$N_z = 6$	$\hat{\tau}_{1 0}^{bc}(h_n, b_n)$	0.00	0.14	0.13	0.93	1146.58	1612.15	1.00
	$\hat{\tau}_{10 00}^{bc}(h_n, b_n)$	0.01	0.39	0.36	0.93	172.69	236.78	1.00
	$\hat{\tau}_{01 00}^{bc}(h_n, b_n)$	0.01	0.49	0.44	0.93	672.35	417.22	0.27
$N_z = 8$	$\hat{\tau}_{1 0}^{bc}(h_n, b_n)$	0.00	0.11	0.11	0.96	1533.33	2155.76	1.00
	$\hat{\tau}_{10 00}^{bc}(h_n, b_n)$	0.03	0.48	0.42	0.92	108.39	148.17	1.00
	$\hat{\tau}_{01 00}^{bc}(h_n, b_n)$	0.05	0.61	0.52	0.91	518.58	277.10	0.19

Table B.3: Simulation results for Scenario B over one thousand replications. S.D. = empirical standard error. S.E. = estimated standard error. C.R. = coverage rate. $N_{d,g}$ and $N_{d',g'}$ = effective sample size on each side of the treatment boundary.

Scenario B - Fixed sample size $N = 3000$

		Bias	S.D.	S.E.	C.R.	$N_{d,g}$	$N_{d',g'}$	Common
$N_z = 3$	$\hat{\tau}_{1 0}^{bc}(h_n, b_n)$	0.00	0.27	0.25	0.94	560.42	780.39	1.00
	$\hat{\tau}_{10 00}^{bc}(h_n, b_n)$	0.00	0.40	0.37	0.93	262.22	361.62	1.00
	$\hat{\tau}_{01 00}^{bc}(h_n, b_n)$	0.00	0.41	0.38	0.93	545.68	548.76	0.63
$N_z = 4$	$\hat{\tau}_{1 0}^{bc}(h_n, b_n)$	-0.02	0.23	0.22	0.95	562.17	783.28	1.00
	$\hat{\tau}_{10 00}^{bc}(h_n, b_n)$	-0.01	0.43	0.39	0.93	179.63	246.41	1.00
	$\hat{\tau}_{01 00}^{bc}(h_n, b_n)$	0.00	0.48	0.44	0.94	508.89	409.32	0.44
$N_z = 5$	$\hat{\tau}_{1 0}^{bc}(h_n, b_n)$	0.01	0.21	0.20	0.95	563.70	786.60	1.00
	$\hat{\tau}_{10 00}^{bc}(h_n, b_n)$	0.01	0.51	0.44	0.91	123.21	167.81	1.00
	$\hat{\tau}_{01 00}^{bc}(h_n, b_n)$	0.01	0.59	0.52	0.92	424.33	294.03	0.33
$N_z = 6$	$\hat{\tau}_{1 0}^{bc}(h_n, b_n)$	-0.01	0.20	0.19	0.94	570.71	799.05	1.00
	$\hat{\tau}_{10 00}^{bc}(h_n, b_n)$	-0.02	0.54	0.50	0.94	83.88	114.05	1.00
	$\hat{\tau}_{01 00}^{bc}(h_n, b_n)$	-0.02	0.71	0.61	0.91	328.61	203.97	0.27
$N_z = 8$	$\hat{\tau}_{1 0}^{bc}(h_n, b_n)$	0.00	0.19	0.18	0.96	566.60	793.13	1.00
	$\hat{\tau}_{10 00}^{bc}(h_n, b_n)$	-0.04	0.75	0.67	0.92	38.59	52.57	1.00
	$\hat{\tau}_{01 00}^{bc}(h_n, b_n)$	-0.05	1.19	0.82	0.84	179.84	99.65	0.19

Table B.4: Simulation results for Scenario B over one thousand replications. S.D. = empirical standard error. S.E. = estimated standard error. C.R. = coverage rate. $N_{d,g}$ and $N_{d',g'}$ = effective sample size on each side of the treatment boundary.